

Technical University Berlin  
Telecommunication Networks Group

---

## Wireless Channel Models

Ana Aguiar, James Gross

{aaguiar,gross}@ee.tu-berlin.de

Berlin, April 2003

TKN Technical Report TKN-03-007

---

TKN Technical Reports Series  
Editor: Prof. Dr.–Ing. Adam Wolisz

## **Abstract**

In this technical report analytical models of wireless channels are presented. The report addresses the reader interested in the various effects, which lead to the well known, unreliable and stochastic nature of wireless channels. The report is composed from various other books, reports and so, due to the reason that a comprehensive, but still easy understandable discussion of the matter for engineers working on protocols is hard to find. Instead many other presentations are quite specific, deal only with a certain amount of the topic, or do not give a certain required level of detail on the other hand.

The report gives an insight into the matter of what influences the performance of wireless channels. Two major effects are distinguished in the report: multiplicative effects, attenuating the transmitted signal, and additive effects, distorting the received signal at the receiver. While the attenuating effects not always have to be considered as stochastic processes, the distorting effects are always of that kind. However, for all effects good mathematical representations are found, which might be utilized for considering the system performance by simulation or analysis. Furthermore, at the end this report, we also briefly give an example analysis of the performance of some digital wireless modulation channels.

# Contents

<b>1</b>	<b>Introduction</b>	<b>3</b>
<b>2</b>	<b>Radio Channel</b>	<b>7</b>
2.1	Path Loss . . . . .	7
2.1.1	Antennas . . . . .	8
2.1.2	Free-Space Propagation . . . . .	8
2.1.3	Two-ray Model . . . . .	9
2.1.4	Empirical and Semi-empirical Models . . . . .	13
2.1.5	Other Models and Parameters . . . . .	16
2.2	Shadowing . . . . .	17
2.2.1	Shadowing Model . . . . .	17
2.2.2	Measurement Results . . . . .	18
2.2.3	Shadowing Correlation . . . . .	18
2.3	Fading . . . . .	20
2.3.1	Physical Basis . . . . .	20
2.3.2	Mathematical Model of Fading . . . . .	22
2.3.3	Characterization in Time and Frequency . . . . .	24
2.3.4	First Order Statistics . . . . .	27
2.3.5	Second Order Statistics . . . . .	30
2.3.6	Fading Rate and Duration . . . . .	36
<b>3</b>	<b>Modulation Channel</b>	<b>40</b>
3.1	Noise . . . . .	40
3.1.1	Thermal Noise . . . . .	40
3.1.2	Filtered White Gaussian Noise . . . . .	41
3.1.3	Man-made Noise . . . . .	42
3.1.4	Some Results . . . . .	42
3.2	Interference . . . . .	43
<b>4</b>	<b>Digital Channel</b>	<b>45</b>
4.1	Structure of the Digital Channel . . . . .	45
4.2	Calculation of the Bit Error Probability as a function of SNIR for Binary PAM over an AWGN Channel . . . . .	46
4.3	Calculation of the Bit Error Probability as a function of SNIR for BPSK over a Rayleigh Fading Channel . . . . .	48

4.4 Results for Other Digital Modulation Schemes over an AWGN Channel . . .	48
<b>5 Conclusions</b>	<b>50</b>

# Chapter 1

## Introduction

The performance of any communication system is ultimately determined by the medium utilized. This medium, may it be an optical fiber, a hard disk drive of a computer or a wireless link, is referred to as **communication channel**. There exists a large variety of channels, which may be divided into two groups. If a solid connection exists between transmitter and receiver, the channel is called a **wired channel**. If this solid connection is missing, this connection is called a **wireless channel**. Wireless channels differ a lot from wired channels, due to their unreliable behavior compared to wired channels. In wireless channels the state of the channel may change within a very short time span. This random and drastic behavior of wireless channels turns communication over such channels into a difficult task.

Wireless channels may be further distinguished by the **propagation environment** encountered. Many different propagation environments have been identified, such as urban, suburban, indoor, underwater or orbital propagation environments, which differ in various ways.

In this report we focus on the factors which influence the performance of wireless channels. We consider analytic models of basic propagation effects encountered in wireless channels and show how they translate into the performance of different communication systems. For example this knowledge is crucial in order to design and parameterize simulation models of wireless channels. A different area where this knowledge is important is the design of communication protocols. In general we address the reader who is interested in the analysis behind wireless channel.

There are multiple books which include various aspects of wireless channels, such as [4, 12, 13, 8, 17, 9, 3]. However, some lack a certain degree of precision when someone is interested in modelling correlated fading on a wireless channel for example. On the other hand some books deal only with some effects, while leaving out other aspects. Also some sources have a degree of detail which is much too high for engineers working on protocol design. Therefore this report has been compiled from various sources, giving a detailed introduction to the main effects one has to consider when dealing with wireless channels in order to evaluate communication protocols. Also we present numerical values for many different situations, such that someone interested in simulating a certain scenario has an easy and complete access to typical values fitting his scenario.

It is not always clear what is referred to as wireless channel in a communication system since there are multiple instances in the transmission and reception process of a signal. Figure

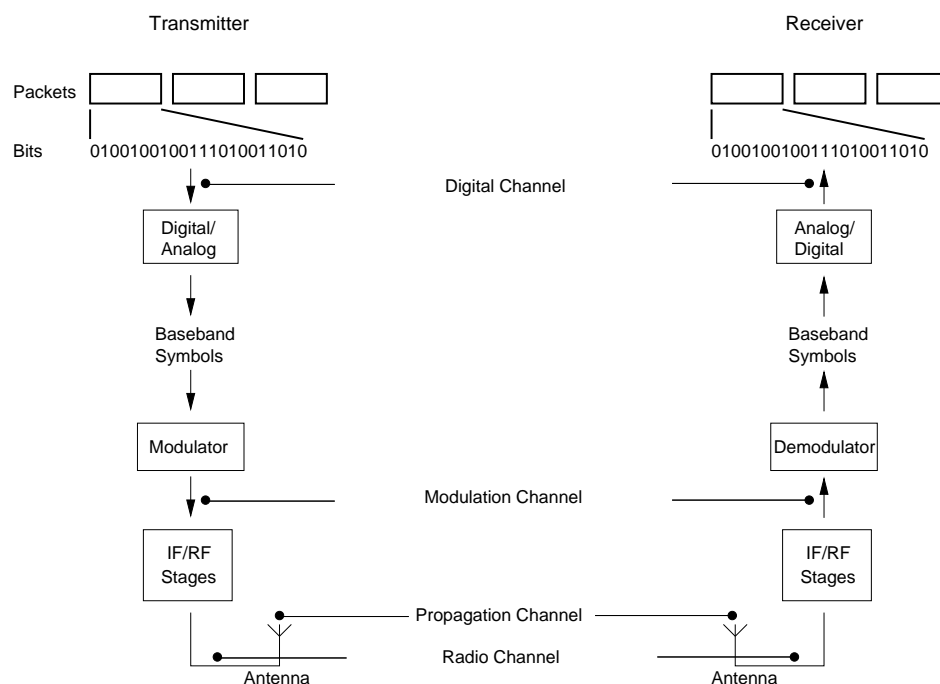


Figure 1.1: Channel classification: propagation channel, radio channel, modulation channel, and digital channel.

1.1 represents the most commonly referenced channels (as referred in [18]) to clarify different notions related to the concept of wireless channels in digital communication systems.

- The **propagation channel**: lies between the transmitter and receiver antennas and is influenced only by the phenomena that influence the propagation of electromagnetic waves. It is almost always linear and reciprocal so that these characteristics will be assumed. All phenomena of this channel only effect the attenuation of the transmitted signal and therefore this channel has an multiplicative effect on the signal. The signal transmitted consists of the information modulated on top of the carrier frequency.
- The **radio channel**: consists of the propagation channel and both the transmitter and receiver antennas. As long as the antennas are considered to be linear, bilateral and passive, the channel is also linear and reciprocal. Still the signal is only effected by attenuation, however the attenuation of the propagation channel might be different since it might be modified by the used antennas, where the antenna influence is strictly linear. The signal transmitted here is the same as with the propagation channel, however it might be scaled by the use of antennas.
- The **modulation channel**: consists of the radio channel plus all system components (like amplifiers and different stages of radio frequency circuits) up to the output of the modulator on the transmitter side and the input of the demodulator on the receiver side. Whether the system is linear depends on the transfer characteristics of the components

between de- or modulator and the antennas. The channel is also non-reciprocal, because amplifiers (the system component added to the radio channel) are non-reciprocal. Due to the process of amplifying the received signal at this point, additive effects damaging the signal come here into play. These are noise and interference. They might already be present at the radio channel, however especially noise from electric circuits is added at this channel level, therefore a complete characterization of the additive effects can not be done at the radio channel level. The signal consists here of the baseband symbols, which are modulated on top of the carrier frequency (refer to next paragraph).

- The **digital channel**: consists of the modulation channel plus the modulator and demodulator. It relates the digital baseband signal at the transmitter to the digital signal at the receiver, and describes the bit error patterns. The channel is non-linear and non-reciprocal. At this channel level no further effects come into play, instead the corrupted signal is interpreted at this level as bit sequence and if the signal has been corrupted too heavily, the interpreted bit sequence differs from the true bit sequence intended to convey. The input to this channel are **bits**, which might stem from packets. The bits are grouped then and turned into analog representations, so called **symbols**. These symbols belong to the baseband. This analog signal is then passed to a modulator, which modulates these baseband signals on top of the carrier frequency.

Assuming ideal antennas, the propagation channel becomes identical to the radio channel. The radio channel attenuates the received signal by a time varying factor, denoted by  $a(t)$ . This attenuation might be compensated by the modulation channel, since amplifiers are employed here to boost the received signal. However, at the modulation channel random, time varying **noise**  $n(t)$  also enters the system, which adds a distorting element to the signal. If the attenuated signal is largely amplified, the noise will also be amplified strongly. Therefore it is up to reliable detection methods at the digital channel to extract the transmitted signal from the noise. In addition to noise, which is always present at this stage of a communication system, it is also possible that electromagnetic waves from other communicating devices interfere with the received signal. This is called **interference** and has a significant impact on the performance, similar to noise. The interfering signal is also time variant and is denoted by  $j(t)$ . The resulting mathematical model of the received signal  $y(t)$ , depending on the sent signal  $s(t)$  and all influencing factors is given in Figure 1.2 (see also [4, 12, 17]).

For a running digital communication system a couple of performance metrics are of common use, such as the **symbol error probability (SEP)** or the **bit error probability (BEP)**. Both performance metrics relate to the digital channel, the BEP relates to the interpreted bit stream, while the SEP relates to the stream of symbols, not being interpreted yet. Both metrics depend on the **instantaneous power ratio** between the received signal power  $y^2(t)$  and the noise and interference powers  $n^2(t)$  and  $j^2(t)$ . This instantaneous power ratio is given by the **Signal-to-Noise-and-Interference Ratio (SNIR)**. Note that the attenuating influence of the radio channel is already included in the received signal power  $y^2(t)$ . A varying SNIR might result in a varying SEP or BEP still this is not necessarily so.

If the **average SNIR** of a link is available, also the average error rates like symbol error rate (**SER**) or bit error rate (**BER**) can be obtained. In general the relationship between SNIR and error rates or error probabilities is not linear, instead it is highly complex and depends on a lot of details. Therefore a deep understanding of the influence of all effects

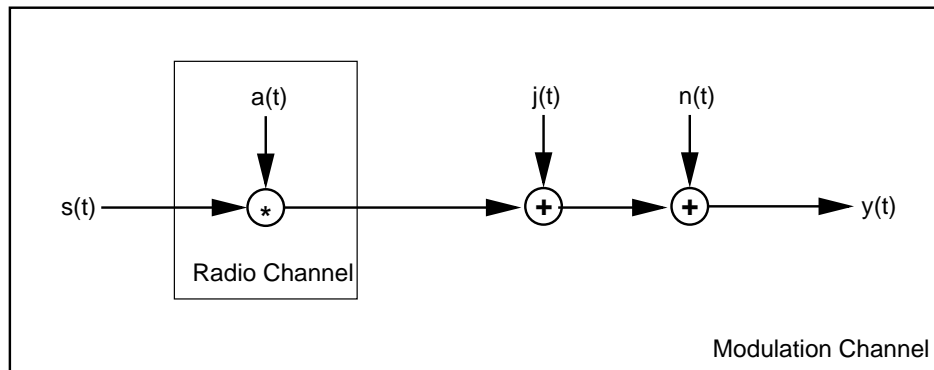


Figure 1.2: Mathematical model of the modulation channel

regarding the receiver SNIR is required for investigations of the performance of any wireless communication systems.

This report is structured as following: we first discuss the effects of the radio channel influencing the signal, therefore at first the attenuation  $a(t)$  is discussed in Chapter 2. Next the noise  $n(t)$  is characterised as well as the interference  $j(t)$ , hence the effects of the modulation channel influencing the signal are discussed in Chapter 3. Finally, we show how these effects influence the received bit stream in the digital channel and therefore have an impact on any of the mentioned performance metrics. This is shown in Chapter 4.

## Chapter 2

# Radio Channel

The radio channel influences the received signal only by a multiplicative factor, the attenuation  $a(t)$ , as given in Figure 1.2. Analytically it is useful to distinguish between three different effects which result in an overall attenuation of the transmitted signal. The first effect is called **path loss**. It is a deterministic effect depending only on the distance between the transmitter and the receiver. It plays an important role on larger time scales like seconds or minutes, since the distance between transmitter and receiver in most situations does not change significantly on smaller time scales. The second effect is called **shadowing**. Shadowing is not deterministic. It varies on the same time scale as the path loss does and causes fluctuations of the received signal strength at points with the same distance to the transmitter. However, the mean over all these points yields the signal strength given by path loss only. The third effect is called **fading**. Fading has also a stochastic nature, but leads to significant attenuation changes within smaller time scales such as milliseconds or even microseconds. Fading is always caused by a multipath propagation environment, therefore by an environment reflecting the transmitted electromagnetic waves such that multiple copies of this wave interfere at the receiving antenna.

All three attenuating effects combined result in the actual experienced attenuation of the radio channel. Therefore this attenuation might be decomposed as given in Equation 2.1 .

$$a(t) = a_{PL}(t) \cdot a_{SH}(t) \cdot a_{FA}(t) \quad (2.1)$$

In the literature shadowing is sometimes also referred to as slow fading while fading is referred to as fast fading in these cases. However, since it is useful to distinguish the phenomenon of fading also into two groups, fast fading and slow fading (Section 2.3.3), we will use throughout this report the terms shadowing and fading to clearly distinguish between them.

### 2.1 Path Loss

In this section the phenomena that influences the propagation of electromagnetic waves will be treated and expressions will be presented for the loss in power that a transmitted signal experiences depending on the distance and frequency. This phenomenon is called path loss.

In general it was said in Chapter 1, that the received signal  $y(t)$  is a stochastic process with average power given by  $\overline{y^2(t)}$ . Since we only deal with the radio channel at this point, the signal of interest at the receiver, will be the signal at the antenna connector without noise, and thus it is given by  $y(t) = a(t) \cdot s(t)$ , while the power of the received signal is given by  $P_0 = \overline{y^2(t)} = \overline{a^2(t) \cdot s^2(t)}$ , where  $P_t = \overline{s^2(t)}$  is the transmitted signal power. We consider as attenuation  $a(t)$  only the component which represents the path loss,  $a_{PL}(t)$ , which is constant in time for a specific non-changing environment, distance and frequency: it is *deterministic*. It follows that  $P_0 = a_{PL}^2(t) \cdot P_t = a_{PL}^2 \cdot P_t$ . This is valid when no movement is assumed: neither the environment is changing nor is the receiver moving. This assumption is equivalent to averaging the smaller scale phenomena in time (shadowing and fading) which will be described in the next Sections.

We focus further on deriving path loss formulas and give some examples on how to parameterise these formulas in realistic environments. Before going into path loss details, some considerations about antennas should be made.

### 2.1.1 Antennas

The function of an **antenna** is to transform electric energy in electromagnetic waves (transmission) and to transform electromagnetic waves back into electromagnetic energy (reception). In the following, we will be talking about conventional antennas: passive and reciprocal (similar characteristics both as transmitter and receiver antenna).

Antennas are characterised by two properties: the gain and the radiation pattern. The **antenna gain** is a measure of the signal amplification introduced by a specific antenna compared to a reference antenna (a dipole). The **antenna pattern** describes the variations of the antenna gain with direction, with reference to the antenna itself. The antenna pattern is usually represented by an attenuation with respect to the maximum antenna gain. The antenna gain and pattern are the same both for transmission and reception.

Antennas can be classified as omnidirectional or directional, depending on whether the gain remains constant in every direction or not, respectively.

When antennas are directional, the antenna pattern has to be taken into account when doing path loss calculations. The value of the gain to be used is the one of the direction of the straight line which connects transmitter and receiver. The antenna gain is then

$$g = G_{max}[dB] - G_{att}^{[Tx Rx]}[dB]$$

, where  $G_{max}$  is the antenna gain and  $G_{att}^{[Tx Rx]}$  is the value from the radiation pattern in the direction of the straight line connecting transmitter and receiver (both in dB); the negative sign is due to the antenna pattern being given as an attenuation with respect to the maximum antenna gain.

### 2.1.2 Free-Space Propagation

The attenuation a signal suffers from propagating in free space over a distance  $d$  between two antennas assuming **line of sight**—**LOS**<sup>1</sup>—, usually named free space path loss, can be

---

<sup>1</sup>LOS: no objects obstructing the path between transmitter and receiver

exactly calculated using the Maxwell equations to calculate the far field of an antenna and is given by [8]

$$\frac{P_0}{P_t} = \left( \frac{\lambda}{4\pi d} \right)^2 g_{Tx} g_{Rx},$$

or in dB

$$\frac{P_0}{P_t} [dB] = 10 \log \frac{P_0}{P_t} = 20 \log \left( \frac{\lambda}{4\pi d} \right) + 10 \log(g_{Tx}) + 10 \log(g_{Rx}),$$

where  $P_0$  is the received power,  $P_t$  is the transmitted power,  $\lambda$  is the wavelength,  $g_T$  is the gain of the transmitter antenna and  $g_R$  is the gain of the receiver antenna (both gains in the direction of the straight line that connects the two antennas in space, see Section 2.1.1). The received power is inversely proportional to the square of the distance and the square of the frequency. The physical explanation for the first is quite straightforward: in free space (no obstacles or reflecting surfaces) the radiated energy propagates equally in every direction and the wave can be seen as a sphere of increasing radius. Since energy cannot be destroyed, it will be the same whatever the distance from the radiating point is. So that the total energy over the sphere is the same independent of the radius, the energy per unit surface must decrease. As the surface increases with the square of the radius, so does energy per unit surface decrease at the inverse rate.

### 2.1.3 Two-ray Model

Since most communications happen close to the earth surface, the scenario for free-space loss is unrealistic. The two-ray model, also known as plane earth, is a simple model based on physical-optics theory which takes the reflection on the earth surface into account. It also assumes LOS and no influence on propagation besides the earth surface. It is a useful starting point for the study of propagation for personal communications. It is often used to describe propagation over water or over open fields.

For its derivation, three waves should be considered: the direct one, one reflected on the earth, and a surface wave. The latter becomes insignificant a few wavelengths above the earth surface and is not significant for mobile communications. It will therefore be neglected.

The following expressions can easily be calculated from the geometry of the model shown in Figure 2.1.

$$\begin{aligned} d1 &= \sqrt{(h_{Tx} - h_{Rx})^2 + d^2} \\ d2 &= \sqrt{(h_{Tx} + h_{Rx})^2 + d^2} \\ \alpha &= \arctan \frac{h_{Tx} - h_{Rx}}{d} \end{aligned}$$

From the free space propagation expression, the power of the direct wave at the receiver is also easily calculated:

$$P_{R1} = P_t \left( \frac{\lambda}{4\pi d1} \right)^2 g_{Tx} g_{Rx}$$

The power of the wave reflected on the earth at the receiver is calculated using the laws of reflection of plane waves [9, 4]. An approximation is needed, since the reflection factors

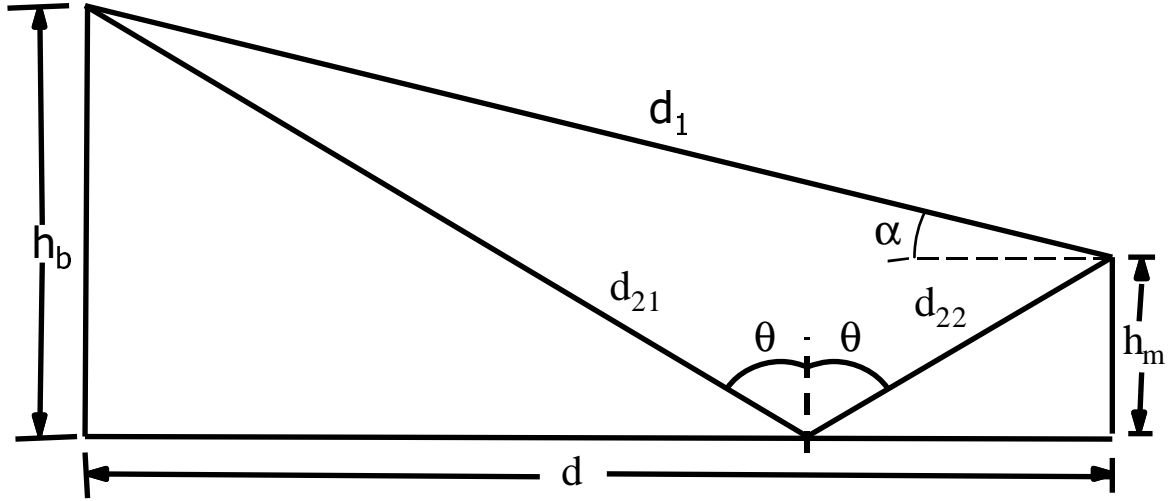


Figure 2.1: Geometry for the calculation of propagation over plane earth (two-ray model).

used are actually calculated for plane waves although the wave is spherical. The reflection factor for an incident wave from vacuum into a surface of electromagnetic properties  $\epsilon_{eff}$  (and magnetic permeability 1 — no magnetic properties), which sets together the conductivity and permittivity of the material is given by

$$R(\theta, \epsilon_{eff}) = \frac{\cos \theta - \sqrt{\epsilon_{eff} - \sin^2 \theta}}{\cos \theta + \sqrt{\epsilon_{eff} - \sin^2 \theta}}.$$

Now the power from the reflected wave at the receiver can be written as a function of known parameters:

$$P_{R2} = P_t R(\theta, \epsilon_{eff}) \left( \frac{\lambda}{4\pi d_2} \right)^2 g_{Tx} g_{Rx}$$

The total power received is then given by

$$P_R = P_t \left( \frac{\lambda}{4\pi} \right)^2 g_{Tx} g_{Rx} \left| \frac{1}{d_1} + R(\theta, \epsilon_{eff}) \frac{e^{j\Delta\Phi}}{d_2} \right|$$

applying the superposition principle to the arriving electric field strengths, where  $\Delta\Phi = 2\pi(d_2 - d_1)\lambda$  is the phase difference between the two waves. An approximation can be made using the Taylor series since  $(d_2 - d_1)$  is very small in the general case (see [9]):  $d_2 - d_1 = \frac{2h_{Tx}h_{Rx}}{d}$ .

Since usually the vertical distance between transmitter and receiver is much smaller than the horizontal one, the approximation  $d = d_1 \approx d_2$  can be used in the fraction terms. The expression can be simplified if the earth surface is considered a metal surface<sup>2</sup> (a very usual

<sup>2</sup>Average ground characteristics are assumed. Electromagnetic characteristics of other types of surface can be found on page 83 of [8].

assumption in electromagnetic calculations) and incidence angles  $\theta$  very near 90 degrees (distance to the reflection point much bigger than height of the transmitter)<sup>3</sup>. In this case, the reflection factor  $R(\theta, \epsilon_{eff})$  takes values very near -1 and a simplified expression for the received power can be written:

$$\begin{aligned} P_0 &= P_t \left( \frac{\lambda}{4\pi d} \right)^2 g_{Tx} \cdot g_{Rx} \cdot 2 \cdot (1 - \cos \Delta\Phi) \\ &= P_t \left( \frac{\lambda}{4\pi d} \right)^2 g_{Tx} \cdot g_{Rx} \cdot 4 \cdot \sin^2 \frac{2\pi h_{Tx} h_{Rx}}{\lambda d} \\ &= P_t \left( \frac{\lambda}{4\pi d} \right)^2 g_{Tx} \cdot g_{Rx} \cdot 4 \cdot \sin^2(\Delta\Phi/2), \text{ for horizontal polarisation} \end{aligned}$$

The approximation for horizontal polarisation in the previous equation is due to the fact that in the real world, most of the time, waves behave like horizontal polarised waves (independently of their actual polarisation).

For values of  $\Delta\Phi$  smaller than 0,6 rad,  $\sin \Delta\Phi/2 \approx \Delta\Phi/2$  and the expression can be further simplified to the known 4th-power-law form:

$$P_0 = P_t \cdot g_{Tx} \cdot g_{Rx} \cdot \left( \frac{h_{Tx} h_{Rx}}{d^2} \right)^2,$$

where the dependence on frequency vanishes.

We calculated the received power  $P_0 = a_{PL}^2 P_t$  as a function of distance according to the three different models seen thus far: the free-space path loss, the two-ray model (with the assumption that the incidence angle is very near 90 degrees), and the 4th power law approximation to the two-ray model. The curves can be seen in Figure 2.2. It can be seen that for the two-ray model there are clearly two different areas: near the transmitter (before the breakpoint), where the received power decreases according to the squared sinus function, with the peak value following the square of the distance; and after the breakpoint, when the phase difference between direct and reflected rays is smaller than 0.6 rad, the second approximation becomes valid, and the received power decreases with the 4th power of the distance (so that the difference between the curves can no longer be seen). The breakpoint can be calculated according to  $d_{Breakpoint} = d|_{\Delta\Phi < 0.6} = \frac{2\pi h_{Tx} h_{Rx}}{0.6 \lambda}$ .

The theoretical results presented have been confirmed by measurements campaigns: results have shown that the 2-ray model fits quite well the actual path loss in line-of-sight (LOS) environments with few or no reflectors and scatterers, e. g. highways (see Section 1.2.6 of [18]).

As was mentioned, the simplified expressions are valid only for very low incidence angles. For steeper incidence angles (transmitter antenna height in the magnitude of the distance) the parameters of the reflecting surface play a determinative role on the propagation and the more accurate expression should be used.

---

<sup>3</sup>Notice also that for frequencies above 100 MHz, changes in the ground parameters do not cause big variations in the path loss [8].

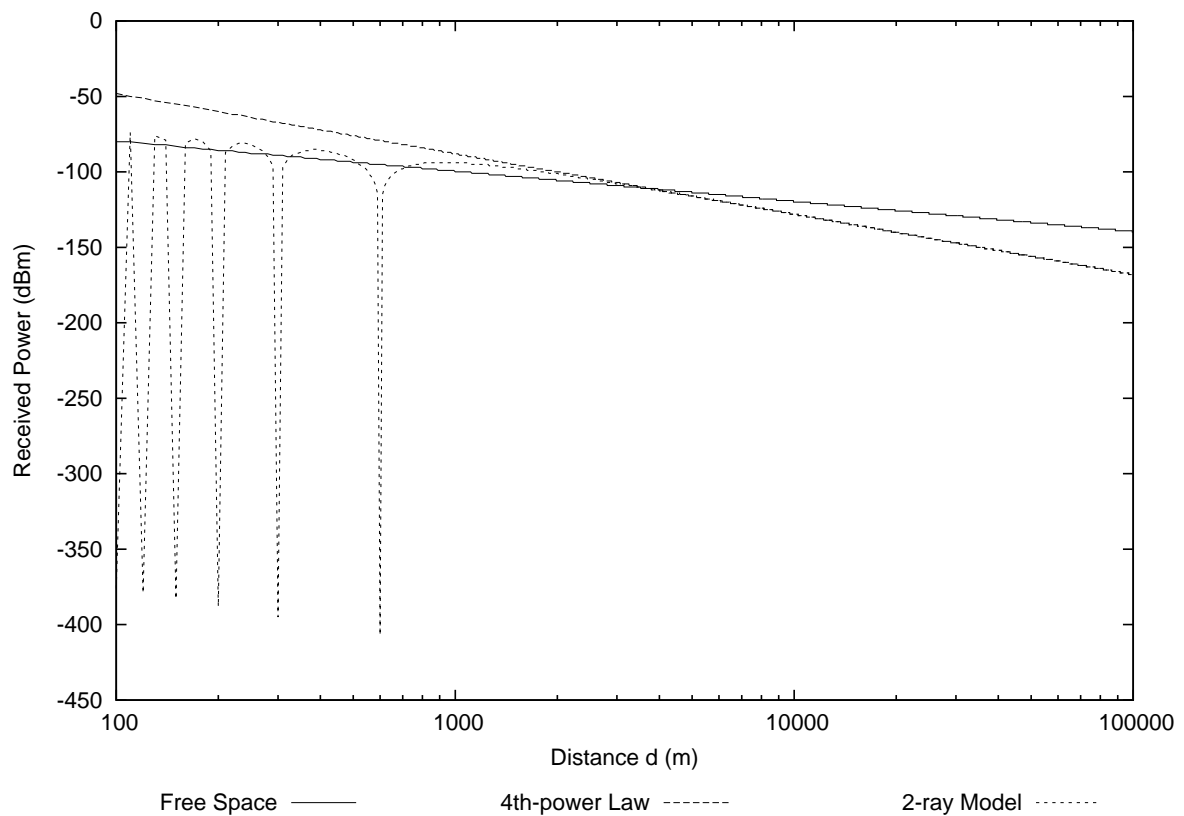


Figure 2.2: Value of the received power  $P_0$  as a function of the distance between transmitter and receiver according to the free space path loss, the two ray model and the 4th-power law. The parameters used are: antennas with unit gain,  $h_{Tx} = 25$  m,  $h_{Rx} = 1.5$  m, transmitted power 0 dBm (1 mW) and 2.4 GHz frequency.

### 2.1.4 Empirical and Semi-empirical Models

For the exact calculations in the previous sections LOS was assumed, as well as no other objects surrounding the path or the transmitter and receiver. These assumptions are not valid in many realistic environments like for urban, suburban and indoor environments, where non-LOS (NLOS) is as common as LOS, a multitude of physical phenomena influence the propagation of electromagnetic waves and the number of possible propagation paths is very high. Ray-tracing models are accurate path loss models, which calculate every possible path between transmitter and receiver, then the attenuation suffered in each path, and finally add all the signal components which arrive at the receiver. These methods not only require exact data about the terrain, the buildings and vegetation but are also very demanding in terms of computing capacity to process all the data and therefore extremely time consuming.

For these reasons, empirical and semi-empirical models have been developed to calculate the path loss between a transmitter and a receiver a certain distance from each other in specific environments for different frequencies. The first are based on extensive measurement campaigns in different environments and the latter on a mix of empirical and theoretical data. For every new area, calibration measurements are required to calculate correction factors for the general models. The models are usually of the form:

$$\frac{P_0}{P_t} = K \cdot \frac{1}{d^\alpha}$$

or, in dB,

$$\frac{P_0}{P_t} [dB] = 10 \log(K) - 10 \cdot \alpha \cdot \log(d)$$

, where the constants  $K$  and  $\alpha$  are fitted to measurement results according to the areas under consideration. The factor  $K$  usually depends on the frequency used, as well as height of the base station and wireless terminal. The distance  $d$  is in units referenced to a reference distance, and has to be defined along with the exponent. Notice that no difference is made between LOS and NLOS anymore, since the models are obtained averaging measurements obtained under both conditions, and the different propagation effects are approximatively condensed in a single parameter —  $\alpha$ .

Some well-known and widely used models are explained next. An overview of other path loss models can be found in [10].

#### The Okumura-Hata Model

The Okumura-Hata model is the most popular of the empirical models. It is based on extensive measurement campaigns made by Okumura in Japan and on a formula developed by Hata which approximates the measured statistics. It is valid for the following values of the parameters:

- frequency: 150...1000 MHz
- distance: 1...20 Km
- Transmitter height over ground: 30...200 m

- Receiver height over ground: 1...10 m

The formula for the path loss is

$$A[dB] = 69.55 + 26.16 \cdot \log(f[MHz]) - 13.82 \cdot \log(h_{Tx}[m]) \\ + (44.9 - 6.55 \cdot \log(h_{Tx}[m])) \cdot \log(d[m]) - \beta ,$$

where  $\beta$  is a correction factor which depends on the environment and takes the following values:

$$\beta = \begin{cases} [1.1 \cdot \log(f[MHz]) - 0.7] \cdot h_{Rx}[m] - [1.56 \cdot \log(f[MHz]) - 0.8] \\ \quad , \text{ for small cities} \\ 8.29 \cdot [\log(1.54 \cdot h_{Rx}[m])]^2 - 1.1 \\ \quad , \text{ for urban areas and } f \leq 300 \text{ MHz} \\ 3.2 \cdot [\log(11.75 \cdot h_{Rx}[m])]^2 - 4.97 \\ \quad , \text{ for urban areas and } f \geq 300 \text{ MHz} \end{cases}$$

For three further environments, further correction factor exist form the corresponding urban formula:

$$\beta_2 = \begin{cases} \beta_{urban} - 2 \cdot [\log(f[MHz]/28)]^2 - 5.4 \\ \quad , \text{ for suburban areas} \\ \beta_{urban} - 4.78 \cdot [\log(f[MHz])]^2 + 18.33 \cdot \log(f[MHz]) - 35.94 \\ \quad , \text{ for almost open rural areas} \\ \beta_{urban} - 4.78 \cdot [\log(f[MHz])]^2 + 18.33 \cdot \log(f[MHz]) - 40.94 \\ \quad , \text{ for open rural areas} \end{cases}$$

This model has been extended by COST (European Cooperation in the Field of Scientific an Technical Research) to COST 231-Hata for frequencies between 1500 MHz and 2000 MHz:

$$A[dB] = 46.3 + 33.9 \cdot \log(f[MHz]) - 13.82 \cdot \log(h_{Tx}[m]) \\ + [44.9 - 6.55 \cdot \log(h_{Tx}[m])] \cdot \log(d[Km]) - \beta + \begin{cases} 3 & \text{for big city centre} \\ 0 & \text{other cases} \end{cases} \\ \beta = [1.1 \cdot \log(f[MHz]) - 0.7] \cdot h_{Rx}[m] \\ - [1.56 \cdot \log(f[MHz]) - 0.8]$$

### The Lee Model

This model [9] is quite popular because its parameters can easily be adapted to a new environment using measurement results. The model consists of two parts:

- the point-to-point model which takes the terrain into account;
- the area-to-area model based on the previous one, which reflects the effects of constructions.

The area-to-area model is similar to the Hata model (Section 2.1.4), where the parameters can easily be found by measurements in the area of interest. Since the area-to-area model reflects the effects of the man-made constructions, if the terrain is hilly, for every distance, measurements have to be made at different terrain heights. The parameters are always the calculated average values from the measurements. Since the measurements are made for certain specific values of antenna height, transmitted power and antenna gain, the model formula has to be corrected to refer the actual used parameters to the ones used in the measurements.

The point-to-point part of Lee's model takes the terrain effects into account, using the effective antenna height<sup>4</sup> and diffraction losses, depending on the situation. The dependance on the effective antenna height is taken from the two-ray model to be of 20 db/dec. The calculation of the effective antenna height used in the expression for the path loss depends on the path under consideration, specifically, on whether it is obstructed or not. In the first case it will be calculated using knife-edge diffraction rules, on the latter using image rule from a two-ray model. The calculation of the effective antenna height is explained in detail in Section 4.7 of [9] and depends on whether a line of sight path is available or not.

$$\begin{aligned}
 P_0 = P_{r0} & - 10 \cdot \alpha \cdot \log(d) + 20 \cdot \log \frac{h'_e}{h_1} + CF \\
 & , \text{ for a path without obstructions} \\
 P_0 = P_{r0} & - 10 \cdot \alpha \cdot \log(d) + 20 \cdot \log \frac{h''_e}{h_1} + L + CF \\
 & , \text{ for an obstructed path and } h''_e \geq 1 \\
 P_0 = P_{r0} & - 10 \cdot \alpha \cdot \log(d) + L + CF \\
 & , \text{ for an obstructed path and } h''_e \approx 1 \\
 P_0 = P_t & - 20 \cdot \log \left( \frac{\lambda}{4\pi d} \right) + 10 \cdot \log(g_{Tx}) + 10 \cdot \log(g_{Rx}) \\
 & , \text{ for propagation over a water surface,}
 \end{aligned}$$

where the first terms  $P_{r0} - 10 \cdot \alpha \cdot \log d$  account for the loss due to human-made structures (parameters taken from measurements) and  $d$  refers to the distance used to calculate the exponent of the path loss,  $CF$  is the correction factor which has the constants due to referring actual parameters to the ones used for model calibration,  $h'_e$  and  $h''_e$  are effective heights for the LOS and non-LOS situations, and  $L$  is the loss due to knife-edge diffraction. Vegetation loss can be added to any of the expressions depending on the situation.

According to Lee [9], the use of the point-to-point models reduces the standard deviation of the predicted values to 3 dB, from the value of 8 dB usually obtained with the area-to-area model. This model is only valid for big distances (above 1 Km) since for lower distances street orientation and buildings can cause very big deviations on actual values and calibration measurement are no longer statistically representative.

---

<sup>4</sup>Effective antenna height is the height of the transmitter antenna referred to the height of the receiver antenna

City	Used antenna height (m)	$\alpha$
Hamburg	40	2.5
Stuttgart	23	2.8
Dusseldorf	88	2.1
Frankfurt	20	3.8
Frankfurt	93	2.4
Kronberg	50	2.4

Table 2.1: Path loss exponent measured in 4 european cities at 900 MHz for a reference distance of 100 m (source [15, 14]).

Environment	Model Type	Used antenna height (m)	$\alpha$	$10 \cdot \log K$ [dB]
Urban	LOS	4	1.4	58.6
Urban	NLOS	4	2.8	50.6
Urban	LOS	12	2.5	35.8
Urban	NLOS	12	4.5	20.0
Urban	LOS	45	3.5	16.7
Urban	NLOS	45	5.8	-16.9
Suburban	LOS	12	2.5	38.0
Suburban	NLOS	5	3.4	25.6
Rural	LOS	55	3.3	21.8
Rural	NLOS	55	5.9	-27.8

Table 2.2: Parameters of the general path loss model from measurements in Finland for 5.3 GHz and a reference distance of 1 m(source [21]).

### 2.1.5 Other Models and Parameters

Besides the models described previously, measurement campaigns have been made in different environments in several countries to better adapt the parameters of the general model form to the real propagation environment, since building materials, urban planning and vegetation differ from country to country.

In [11] measurement done in Tokio for frequencies ranging from 457 MHz to 15.45 GHz have shown that the frequency dependency of the path loss in the UHF band ([300;3000] MHz) follows the free-space trend of  $20 \cdot \log(f)$ .

Best-fit parameters for measurements made in european cities for 900 MHz and a reference distance of 100 m can be found in [15, 14] (see Table 2.1).

In [16] the value of  $\alpha$  for 3.5 GHz in a dense urban environment is found from measurements to be 4.7-4.8.

Results of path loss model parameters obtained from a least square analysis of measurement results in several environments at 5,3 GHz in outdoor urban, suburban and rural environments are presented in [21] — see Table 2.2.

The models presented and referred in this short survey are for the frequency ranges in which

wireless LANs and HiperLAN operate (2,4-5 GHz). It is not pretended to list all existing models, but to give a short overview of the different possibilities and of the parameters which influence both propagation and model development and choice.

The models presented are from the author's point of view the most meaningful in the UHF and VHF frequency bands, either because they are widely accepted, or because they are representative of other models. Several other models exist for other frequencies and environments, which are certainly not less important, but are out of the scope of this short survey.

## 2.2 Shadowing

The path loss model presented in the previous section aims at a deterministic calculation of the path loss for a determined position of transmitter and receiver. In reality the position of a receiver involves also the objects surrounding the transmission path as well as the terrain. Measurements have been made under several different conditions and statistical variations have been observed. For a fixed frequency and distance, different values of the received signal power were measured. Thus, for a given fixed distance, frequency and transmission power, the received signal power is not deterministic, but varies due to the objects in and around the signal path. These stochastic, location dependent variations are called shadowing and were denoted in Equation 2.1 by  $a_{SH}(t)$ . Note that these stochastic variations are constant in time, as long as the receiver and his complete environment do not move. Shadowing reflects the differences in the measured received signal power with relation to the theoretical value calculated by path loss formulas. Averaging over many received signal power values for the same distance, however, yields the exact value given by path loss.

Note that shadowing is an abstraction which reflects the result of a sum of several propagation phenomena which occur when an electromagnetic wave propagates in an environment: reflections (e. g. on buildings and ground), diffraction (e. g. around buildings), refraction (e. g. through walls or windows), scattering (e. g. on buildings, trees or ground) and absorption (e. g. on forest or parks)<sup>5</sup>. The calculation of the effects of every of these phenomena for each location is not feasible (sometimes even impossible) both due to complexity and time limitations. Therefore, shadowing is used to describe the aggregated effects of all these phenomena.

The objects causing these variations are of such dimensions that a receiver moving along a line at constant distance from the transmitter will take several hundreds of milliseconds (ms) to move to an area with different characteristics.

### 2.2.1 Shadowing Model

From measurements of path loss for a variety of environments and distances, the variations of the measured signal level relative to the average predicted path loss were calculated (see figures 2.37 to 2.41 from [18]). Its distribution is normal with 0 mean in dB, which implies a log-normal distribution of the received power around the mean value corresponding to

---

<sup>5</sup>Note that, although the term shadowing comes from diffraction around buildings (a non LOS situation), it is also present in LOS situations (see the measurements results shown in ...

City	Used antenna height (m)	$\sigma_{SH}$ [dB]
Hamburg	40	8.3
Stuttgart	23	9.6
Dusseldorf	88	10.8
Frankfurt	20	7.1
Frankfurt	93	13.1
Kronberg	50	8.5

Table 2.3: Standard deviation of the path loss measured in european cities at 900 MHz (source [15, 14])

the path loss. This hypothesis has been verified with the  $\chi^2$  and Kolmogrov-Smirnov test and found to be valid with high confidence intervals. The theoretical basis to the log-normal distribution is that in an environment with surrounding objects different signals suffer random reflections and diffractions as they traverse the propagation medium. Expressed in dB, the extra loss in each path corresponds to subtracting a random loss from the path loss value. As the different propagation paths are independent, the sum of all the dB losses for a large number of propagations path converges to a normally distributed random variable (central limit theorem). In natural units, that becomes a log-normal distribution.

The shadowing variations of the path loss can therefore be calculated from the distribution

$$p(a_{SH}) = \frac{1}{\sigma_{SH}\sqrt{2\pi}} \exp -\frac{a_{SH}^2}{2\sigma_{SH}^2},$$

where  $\sigma_{SH}$  is the variability of the signal and all variables are expressed in dB.

The value of the variation due to shadowing is then added to the path loss value to obtain the variations.

$$a[dB] = 10 \cdot \log \frac{P_0}{P_i} = a_{PL}[dB] + a_{SH}[dB]$$

### 2.2.2 Measurement Results

The standard deviation of  $a_{SH}$ ,  $\sigma_{SH}$ , usually takes values between 5 dB and 12 dB [20], depending on the communications system used (value is chosen based on extensive measurement campaigns). For cellular communication networks a value of 7-8 dB [9, 19] taken from several measurements is usually used.

Measurement campaigns have been made in several different environments and some results for the standard deviation  $\sigma_{SH}$  are presented here.

In [16]  $\sigma_{PL_{SH}}$  is found to be around 6.12 dB for a dense urban environment at 3.5 GHz.

Some values of the standard deviation of the path-loss from measurement results at 5,3 GHz in outdoor urban, suburban and rural environments are presented in Table 2.5.

### 2.2.3 Shadowing Correlation

The autocorrelation of the shadowing process in space also needs to be modelled, since values at close locations are expected to be correlated. A simple negative exponential correlation

Frequency (MHz)	Average building height(m)		
	30	20	20
457.2	8.62	6.34	6.89
813	—	5.10	—
2200	7.29	5.59	7.56
8450	7.98	5.48	7.21
15450	7.45	5.2	6.82

Table 2.4: Standard deviation of the path loss measured in Tokio at several UHF frequencies for different environments, here for BS-WT distance lower than 1 Km and BS antenna height above rooftops (see source [11] for further results)

Environment	Model Type	Used antenna height (m)	$\sigma_{PL_{SF}}$ [dB]
Urban	LOS	4	3.7
Urban	NLOS	4	4.4
Urban	LOS	12	2.9
Urban	NLOS	12	1.7
Urban	LOS	45	4.6
Urban	NLOS	45	2.8
Suburban	LOS	12	4.9
Suburban	NLOS	5	2.8
Rural	LOS	55	3.7
Rural	NLOS	55	1.9

Table 2.5: Standard deviation of the path-loss from measurements in Finland for 5.3 GHz (source [21]).

model is proposed in [7] to work on an Okumura path loss model:

$$R_{PL}(k) = \sigma_{SH}^2 \cdot a^{|k|} a = \epsilon_D^{\frac{vT}{D}},$$

where  $k$  is the distance between two points in m,  $\epsilon_D$  is the correlation between two points at distance  $D$ ,  $T$  is the interval between samples and  $v$  is the speed of the movement. The parameters of the model —  $a$  and  $k$  — should be fitted to measured values after removal of fast fading variations.

The proposed model has been fitted to data for urban and suburban environments in two European cities. The data for suburban environments was measured at 900 MHz, and  $\sigma_{a_{SH}}$  was estimated to be 7.5 dB and  $\epsilon_D$  0.82 for a distance of 100 m. The urban data was collected for 1700 MHz and the estimated model parameters were 4.3 dB for  $\sigma_{SH}$  and 0.3 for  $\epsilon_D$  for a distance  $D$  of 10 m. The fit in suburban environments is good for distances  $k$  up to 500 m but for urban environments the model departs from the measured values for distances above 15 m. The measured values of autocorrelation in an urban environment are also very low (below 20%) for distances above 13 m (see Figure 2 in [7]). It is suggested that this is due to the fact that fast fading (see next section) was not completely removed of the measurement traces used.

## 2.3 Fading

Fading is the interference of many scattered signals arriving at an antenna. It is responsible for the most rapid and violent changes of the signal strength itself as well as its phase. These signal variations are experienced on a small time scale, mostly a fraction of a second or shorter, depending on the velocity of the receiver. In this Section we will discuss the physical reasons causing fading, present a mathematical model for fading and characterize it as a stochastic process. Fading might have a time varying or frequency varying attenuating impact on the transmitted signal, denoted by  $a_{FA}(t)$  in Equation 2.1. Due to the frequency varying and time varying (complex valued) nature of fading, we will denote the attenuating impact in this Section by  $\bar{G}(t, f)$ . The relationship to the notation used in Equation 2.1 is given by  $a_{FA}(t) = |\bar{G}(t, f)|$  for the observed carrier frequency. In some cases the fading might be only time varying or frequency varying, in these cases we denote the fading by  $\bar{g}(t) = \bar{G}(t, 0)$  in the case of time varying fading only and by  $\bar{G}(f) = \bar{G}(0, f)$  in the case of frequency varying fading only. The relationship to the notation used in Equation 2.1 is in these cases still given by  $a_{FA}(t) = |\bar{G}(t, f)|$  for the observed carrier frequency.

In the following we will first introduce a mathematical model, which allows the an analytical study of multipath propagation and fading. Then we will discuss first and second order statistics of fading as well as methods in order to characterize fading channels and certain parameters describing the severeness of the fading channel. Most of this is following the chapter about fading in [4].

### 2.3.1 Physical Basis

The physical basis of fading is given by the reception of multiple copies of the transmitted signal, each having followed a different path. Depending on the environment of transmitter

and receiver, there can be many or only few objects reflecting the transmitted radio signal. In general these objects are known as **scatterers** and the transmission of a signal leads to a situation shown in Figure 2.3, which is called a **multipath signal propagation**.

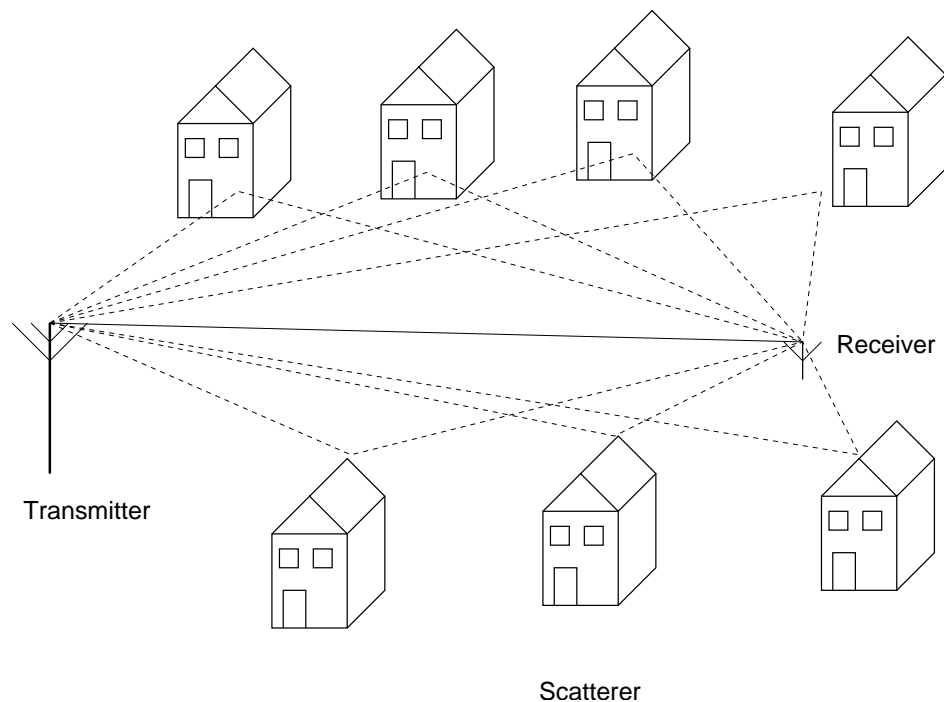


Figure 2.3: Multipath propagation scenario with a transmitter, a receiver and seven scatterers

In a typical environment each path  $i$  has a different length  $l_i$ . Due to this difference in length, each signal travelling along a path arrives with a different **delay**  $\tau_i = \frac{l_i}{c}$ , where  $c$  is the speed of light. Some signal copies travelling along short paths will arrive quite fast, while other copies travelling along longer paths will arrive later. Physically this equals an echo, encountered in a canyon. The channel is said to have a memory, since it is able to store signal copies for a certain time span.

Beside this multipath propagation, each signal copy is attenuated differently, since the signal paths have to pass different obstacles like windows, building walls of different materials, trees of different sizes and so on. Denote the attenuation factor of path  $i$  by  $a_i$ .

Taking all this into account, the multipath propagation of a transmitted radio wave results in an interference pattern, where at certain points the wave interfere constructively while at other points they interfere destructively. If each element within the propagation environment (transmitter, scatterers, receiver) do not move, the receiving signal will only suffer from the **delay spread** and the different attenuation. In this case, the interference situation of the channel stays constant and therefore the channel is said to be **time invariant**. In contrast, if any kind of movement is encountered in the propagation environment, all or some paths change in time, such that all  $a_i$  and  $\tau_i$  change in time. As a consequence the wireless channel become **time variant**. Here, along with a constant changing delay spread, the receiver also

experiences a varying signal strength due to its movement through the interference pattern, therefore the received signal fades.

### 2.3.2 Mathematical Model of Fading

Consider the transmission of a bandpass signal at carrier frequency  $f_c$  with complex envelope  $\bar{s}(t)$ . This transmitted bandpass signal is given by Equation 2.2.

$$s(t) = \text{Re} \left( \bar{s}(t) \cdot e^{2\pi j \cdot f_c t} \right) \quad (2.2)$$

The received bandpass signal is given by Equation 2.3.

$$y(t) = \text{Re} \left( \bar{y}(t) \cdot e^{2\pi j \cdot f_c t} \right) \quad (2.3)$$

We look for a mathematical model of the received bandpass signal taking into account the effect of multipath propagation. At first we consider the case where we do not encounter motion in the environment. As described in Section 2.3.1, each path is associated with a different length  $l_i$  and a different attenuation  $a_i$ . Therefore the received signal  $y(t)$  is the superposition of all copies, given in Equation 2.4.

$$y(t) = \sum_{\forall i} a_i \cdot s \left( t - \frac{l_i}{c} \right) = \text{Re} \left( \sum_{\forall i} a_i \cdot \bar{s} \left( t - \frac{l_i}{c} \right) \cdot e^{2\pi j \cdot f_c \cdot \left( t - \frac{l_i}{c} \right)} \right) \quad (2.4)$$

Considering the relationship between wavelength and frequency  $\lambda = \frac{c}{f_c}$ , we obtain a complex envelope representation in Equation 2.5. Denote by  $\varphi_i = 2\pi \cdot \frac{f_c l_i}{c} = 2\pi \cdot \frac{l_i}{\lambda}$  the phase shift of the carrier frequency caused by the different length of each path. Also recall the introduction of the path delay  $\tau_i = \frac{l_i}{c}$  from Section 2.3.1.

$$\bar{y}(t) = \sum_{\forall i} a_i \cdot e^{-2\pi j \cdot \frac{l_i}{\lambda}} \cdot \bar{s} \left( t - \frac{l_i}{c} \right) = \sum_{\forall i} a_i \cdot e^{-j \cdot \varphi_i} \cdot \bar{s}(t - \tau_i) \quad (2.5)$$

Without motion a multipath environment leads to the interference of multiple copies with a different attenuation of the envelope, respectively the carrier, ( $a_i$ ), a different phase shift of the carrier ( $\varphi_i$ ) and a different delay of the envelope ( $\tau_i$ ).

Now let us consider the effect of motion in this model. Does the motion of the receiver have a great impact on the behavior of the received signal, as described in Section 2.3.1? Denote by  $\gamma_i$  the angle of arrival of path  $i$  with respect to the direction of motion of the receiver, as shown in Figure 2.4.

The path length change, as a function of speed  $v$  and time  $t$  is given by  $\Delta l_i = -v \cdot \cos(\gamma_i) \cdot t$ . From this we obtain a different function for the complex envelope, which depends now on the time  $t$ , as given in Equation 2.6.

$$\begin{aligned} \bar{y}(t) &= \sum_{\forall i} a_i \cdot e^{-2\pi j \cdot \frac{l_i + \Delta l_i}{\lambda}} \cdot \bar{s} \left( t - \frac{l_i + \Delta l_i}{c} \right) \\ &= \sum_{\forall i} a_i \cdot e^{-j \varphi_i} \cdot e^{-2\pi j \cdot \cos(\gamma_i) \cdot t \frac{v}{\lambda}} \cdot \bar{s} \left( t - \tau_i + \frac{v \cdot \cos(\gamma_i) \cdot t}{c} \right) \end{aligned} \quad (2.6)$$

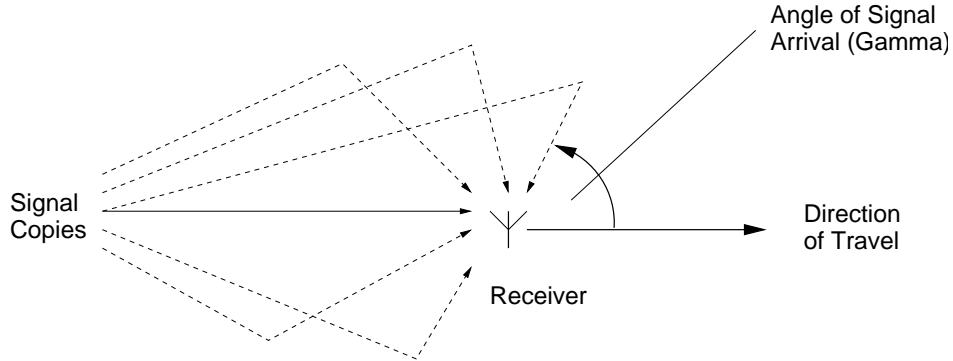


Figure 2.4: Detailed sketch of signal arrival

Equation 2.6 can be simplified. First we include the phase  $e^{-j\varphi_i}$  in  $a_i$ , but indicate this by writing  $\bar{A}_i$  instead. Second, when comparing the delay caused by the term  $v \cdot \cos(\gamma_i)t/c$  with the overall signal length of the complex envelope  $\bar{s}(t)$ , then the delay variation is very short such that it can be ignored. Another simplification is done through introducing the **Doppler frequency**  $f_d = \frac{f_c}{c} \cdot v = \frac{v}{\lambda}$  and the **Doppler shift**  $\nu_i = \cos(\gamma_i) \cdot f_d$ . With this we obtain Equation 2.7.

$$\bar{y}(t) = \sum_{\forall i} \bar{A}_i \cdot e^{2\pi j \cdot \cos(\gamma_i) \cdot t \cdot f_d} \cdot \bar{s}(t - \tau_i) = \sum_{\forall i} \bar{A}_i \cdot e^{2\pi j \cdot \nu_i \cdot t} \cdot \bar{s}(t - \tau_i) \quad (2.7)$$

Interpreting Equation 2.7 yields the following. The motion of the receiver in combination with the  $i$ -th scatterer influences the received signal in the amplitude of the carrier, respectively the envelope and in the phase ( $\bar{A}_i$ ), in the carrier frequency ( $\nu_i$ ) and in the delay of the envelope ( $\tau_i$ ). We have not mentioned the delay change of the envelope, which is relatively small. Therefore motion of the receiver or a scatterer in the model introduces a frequency offset of the carrier in addition to the signal changes that are already present if no motion is involved.

If the number of scatterers is very high, the discrete scatterer model has to be turned into a continuous scatterer model, where each specific scenario is represented by a gain density, given by the **delay-Doppler spread function** in Equation 2.8.

$$\bar{\varrho}(\nu, \tau) d\nu d\tau = \sum_{\forall \hat{i}} \bar{A}_{\hat{i}} \quad (2.8)$$

Here,  $\hat{i}$  indexes all scatterers with delay in  $d\tau$  and Doppler shift in  $d\nu$ . With this the received signal  $\bar{y}(t)$  is given in Equation 2.9.

$$\bar{y}(t) = \int_0^\infty \int_{-f_d}^{f_d} \bar{\varrho}(\nu, \tau) \cdot e^{2\pi j \cdot \nu_i \cdot t} \cdot \bar{s}(t - \tau_i) \cdot d\nu d\tau \quad (2.9)$$

### 2.3.3 Characterization in Time and Frequency

Out of the different impacts on the signal received in a multipath environment including motion, the frequency offset (Doppler shift) of the carrier and the time delay of the envelope damage the signal most. This is because these shifted and delayed waves might interfere destructively and therefore cause severe attenuation. In practice a wireless transmission in a certain environment including a certain velocity of objects is described by two values, the Doppler spread  $\Delta f_d$  and the delay spread  $\Delta\tau$ . Both spreads result from multipath reception (and in the case of the Doppler spread also from the velocity involved), where each path may be characterized by a different Doppler shift (due to a different receive angle) and time delay. While the Doppler spread is caused by the motion of objects within the environment (which might be the transmitter, the receiver or scatterers), the delay spread is caused by the topology of the environment itself. As we will see, although the Doppler spread is a phenomenon in frequency (generating Doppler shift, a shift in frequency), the overall result on the received signal (which is the result of multiple Doppler shifted signal copies interfering) is a time selective behavior. For the delay spread this is exactly the opposite. While the delay spread is a phenomenon in time, the resulting impact on the received signal is a frequency selective behavior. This is now derived from the mathematical model in Section 2.3.2. Here we first start with the discussion of the Doppler spread impact, then the discussion of the delay spread impact follows.

Consider a receiver, which moves through a multipath environment with a certain fixed speed. Further consider all path delays in this environment to be negligible small, such that  $\bar{s}(t - \tau_i) \approx s(t)$ . Then the received complex envelope, given by Equation 2.7, is simplified and turns into Equation 2.10.

$$\bar{y}(t) = \bar{s}(t) \cdot \sum_{\forall i} \bar{A}_i \cdot e^{2\pi j \cdot \cos(\gamma_i) \cdot t \cdot f_d} = \bar{s}(t) \cdot \bar{g}(t) \quad (2.10)$$

Here  $\bar{g}(t)$  is called the **complex gain** of the channel. In this case, the input  $\bar{s}(t)$  and the output  $\bar{y}(t)$  of the channel are connected by a simple multiplicative relationship. Because the phase angles  $2\pi j \cdot \cos(\gamma_i) \cdot t \cdot f_d$  change in time, the channel complex gain is time varying. Considering the transmission of a pure tone (setting the amplitude constant, thus  $\bar{s}(t) = U$ ), the received signal would be spread out in frequency, shifted within the interval  $[-f_d, f_d]$ . Due to this spreading, the received signal  $\bar{y}(t)$ , which consists now of several tones at different frequencies interfering at the receiving antenna, would vary in time. The *wireless channel* therefore becomes **time selective**. At some time instances the received signal is not attenuated and could appear even enhanced, at other time instances the signal is severely attenuated. Thus,  $\bar{g}(t)$  varies in time.

For maximum values of the Doppler shift  $f_d$  at different velocities and different carrier frequencies refer to table 2.6.

The severity of the time selective behavior caused by the Doppler spread depends on the time span the receiver needs to process the incoming envelope at the digital channel (as explained in the introduction). If coherent detection is assumed (where each symbol is processed independently, since transmitter and receiver are perfectly synchronized), the processing time is the length of the envelope itself, which is the symbol length  $T_s$ . If the receiver employs for example differential detection (as with DPSK), the processing time

Carrier Frequency	$f_d @ 1 \frac{m}{s}$	$f_d @ 10 \frac{m}{s}$	$f_d @ 20 \frac{m}{s}$	$f_d @ 100 \frac{m}{s}$
1 Mhz	0.003 Hz	0.033 Hz	0.066 Hz	0.33 Hz
100 Mhz	0.33 Hz	3.33 Hz	6.6 Hz	33 Hz
1 Ghz	3.33 Hz	33.33 Hz	66 Hz	333 Hz
2.4 Ghz	8 Hz	80 Hz	160 Hz	800 Hz
5.4 Ghz	18 Hz	180 Hz	360 Hz	1.8 kHz
10 Ghz	33 Hz	333 Hz	666 Hz	3.33 kHz
60 Ghz	200 Hz	2 kHz	4 kHz	20 kHz

Table 2.6: Doppler shift frequencies for different carrier frequencies at velocities comparable to walking ( $1 \frac{m}{s}$ ), a slow car ( $10 \frac{m}{s}$ ), a fast car ( $20 \frac{m}{s}$ ) and traveling per train (ICE  $100 \frac{m}{s}$ )

equals twice the time span of a symbol, since the receiver always has to take two symbols into account in order to obtain the information. If the receiver also employs an equalizer, a device which tries to revert the attenuating influence of the channel by means of adaptive digital filtering over many symbols, this time span is further increased. In general we represent the processing time span by  $N \cdot T_s$ . If the fade rate of the time selective process given by the Doppler frequency  $f_d$  is larger than the processing rate (given by  $\frac{1}{N \cdot T_s}$ ), then the *fading* is called **time selective**<sup>6</sup>. In contrast, if the fade rate is much lower than the processing rate, therefore if  $f_d \cdot N \cdot T_s \ll 1$ , then the *fading* is called **not time selective**. These two conditions are also named **fast and slow fading**, respectively.

Now let us focus on the impact of delay spread, without the presence of Doppler spread. For a stationary receiver, we can assume the phases of the reflected signal copies to be constant. Therefore we can consider Equation 2.11 as mathematical model.

$$\bar{y}(t) = \sum_{\forall i} \bar{A}_i \cdot \bar{s}(t - \tau_i) = \bar{g}(t) * \bar{s}(t) \quad (2.11)$$

The input is in this case related to the output by convolution with the complex gain  $\bar{g}(t)$ . Since the phases are constant (but still random), the channel might be modelled in this case as **linear, time invariant filter** with an impulse response given in Equation 2.12.

$$\bar{g}(t) = \sum_{\forall i} a_i \cdot e^{-j \cdot \varphi_i} \cdot \delta(t - \tau_i) = \sum_{\forall i} \bar{A}_i \cdot \delta(t - \tau_i) \quad (2.12)$$

In the frequency domain the relationship between input  $\bar{S}(f)$  and output  $\bar{Y}(f)$  is given by multiplication with the frequency response of the filter, the **complex transfer function**  $\bar{G}(f)$ . The transfer function is given in Equation 2.13.

$$\bar{G}(f) = \sum_{\forall i} \bar{A}_i \cdot e^{-2\pi j \cdot f \cdot \tau_i} \quad (2.13)$$

Since the delays  $\tau_i$  are different for several paths, some frequencies are attenuated while others are not. If the delay difference between the paths is very small or even not existing,

---

<sup>6</sup>Note that a channel is always time selective if motion is present, while time selective fading depends on the relationship between symbol time and Doppler frequency

Environment	$\tau_{rms}$
Urban	1 – 25 $\mu$ s
Suburban	0.2 – 2 $\mu$ s
Indoor	25 – 250 ns

Table 2.7: Standard deviation of delay spread values for three often referred transmission environments

Criteria	Category
$\frac{\Delta\tau}{T_s} \ll 1, f_d \cdot T_s \ll 1$	not frequency selective (flat), not time selective (slow)
$\neg \left( \frac{\Delta\tau}{T_s} \ll 1 \right), f_d \cdot T_s \ll 1$	frequency selective, not time selective (slow)
$\frac{\Delta\tau}{T_s} \ll 1, \neg (f_d \cdot T_s \ll 1)$	not frequency selective (flat), time selective (fast)
$\neg \left( \frac{\Delta\tau}{T_s} \ll 1 \right), \neg (f_d \cdot T_s \ll 1)$	frequency selective, time selective (fast)

Table 2.8: Categories in order to characterize the fading of a wireless channel depending on the Doppler and delay spread

then no frequency is attenuated by the delay spread. The severity of the delay spread can be estimated by the product of the required baseband bandwidth of the signal (denoted by  $W$ , and related to the symbol time  $T_s$ ) and the delay spread. If the delay spread is very small compared to symbol time  $T_s$ , then it has almost no impact on the reception of the signal (if  $\Delta\tau \cdot W \ll 1$ ). In this case the transfer function of the channel has no significant attenuating behavior within the bandwidth of the signal  $W$ . The *fading* is called to be **flat or frequency non selective**, since for the utilized frequencies of the channel no signal attenuation is present due to delay spread. On the other hand if the delay spread is significant compared to the symbol time  $T_s$ , then the channel has a **frequency selective** behavior. That is, at some frequencies of the baseband signal the received signal is attenuated while at other frequencies the signal might be enhanced. In this case the receiver suffers in the time domain from **intersymbol interference (ISI)**. If the delay spread is for example half of the symbol time, then signal copies of two consecutively sent symbols interfere at the receiver, such that the 'fast' signal copy of the latter sent symbol interferes with the 'slow' signal copy of the previous sent symbol.

Table 2.7 gives typical ranges for the standard deviation of the delay spread. Note that mean values of the mentioned environments are of no interest, since the variation of delays damages the signal, not a longer or shorter mean delay.

In practical situations most of the time both, Doppler and delay spread, are present. However, both effects can be of harm or not, depending on the ratio between the symbol time (baseband bandwidth) and the characteristic values of the effects  $f_d$  and  $\Delta\tau$ . Therefore, a channel might be categorized into four different types, always depending on the ratios mentioned. The four categories are listed in Table 2.8, assuming coherent detection.

If both kinds of spread are present the channel has to be modelled as **linear time variant filter** (the filter model is necessary due to the delay spread, the time variant behavior is due

to the Doppler spread). In this case input and output of the channel are related by Equation 2.14.

$$\bar{y}(t) = \sum_{\forall i} \bar{A}_i \cdot e^{2\pi j \cdot \nu_i \cdot t} \cdot \bar{s}(t - \tau_i) = \bar{g}(t, \tau) * \bar{s}(t) = \int_0^{\Delta\tau} g(t, \tau) \cdot \bar{s}(t - \tau) d\tau \quad (2.14)$$

The impulse response is given by Equation 2.15.

$$\bar{g}(t, \tau) = \sum_{\forall i} \bar{A}_i \cdot e^{2\pi j \cdot \nu_i \cdot t} \cdot \delta(\tau - \tau_i) \quad (2.15)$$

In the frequency domain, Equation 2.14 turns into Equation 2.16.

$$\bar{Y}(f) = \bar{G}(t, f) \cdot \bar{S}(f) = \sum_{\forall i} \bar{A}_i \cdot e^{2\pi j \cdot \nu_i \cdot t} \cdot e^{-2\pi j \cdot f \cdot \tau_i} \cdot \bar{S}(f) \quad (2.16)$$

Here  $\bar{G}(t, f)$  is called the **time variant transfer function** and determines the gain experienced at time  $t$  to a frequency component at frequency  $f$ . From this function  $\bar{G}(t, f)$ , the complex gain  $\bar{g}(t)$  in the presence of Doppler spread only is obtained by setting the frequency component to zero, hence  $\bar{g}(t) = \bar{G}(t, 0)$ . Accordingly, the complex transfer function in the presence of delay spread only is given by  $\bar{G}(f) = \bar{G}(0, f)$ .

### 2.3.4 First Order Statistics

A received signal consists in general of a large number of signal copies which interfere at the receiver's antenna. The channel could be seen in principle as a deterministic channel, if all reflection coefficients were known at each time instance. Due to the large number of reflection paths this is not possible in practice. Therefore a statistical description is the only way to characterize at least some properties of the channel.

Due to the high number of signal paths existing in a usual transmission environment, the central limit theorem may be applied to the statistical behavior of the interfering signal copies at the receiver. Therefore the complex gain  $\bar{g}(t)$  from Equation 2.10 can be modeled as Gaussian random process in time if Doppler spread is present. If delay spread is present, the complex transfer function  $\bar{G}(f)$  from Equation 2.13 can be modelled as Gaussian random process in frequency. If both kinds of spread are present, the time variant transfer function  $\bar{G}(t, f)$ , the Fourier transform of the time variant impulse response of Equation 2.15, can be modelled as Gaussian random process in both time and frequency.

Assuming the complex gain to be Gaussian (in the case of flat fading and the absence of a line of sight component), the probability density of the complex gain  $\bar{g}(t)$  is given by Equation 2.17 .

$$p(\bar{g}) = \frac{1}{2\pi\sigma_g^2} \cdot e^{-\frac{(|\bar{g}|)^2}{\sigma_g^2}} \quad (2.17)$$

The variance  $\sigma_g^2$  is given by Equation 2.18 .

$$\sigma_{\bar{g}}^2 = \frac{1}{2} \cdot E(|\bar{g}(t)|^2) = \frac{1}{2} \cdot (E(g_r(t)^2) + E(\bar{g}_i(t)^2)) \quad (2.18)$$

Note that the real and imaginary components are individually Gaussian processes. Also the Gaussian process of the complex gain has a mean equal to zero. Figure 2.5 shows a plot of the probability density function.

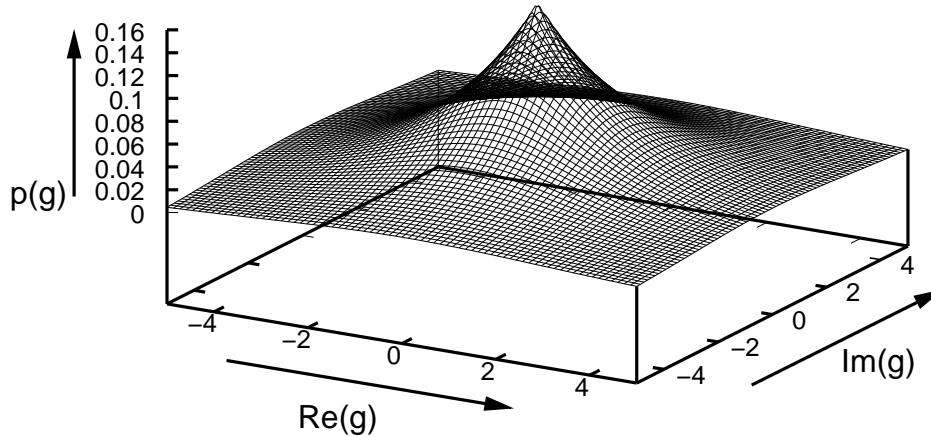


Figure 2.5: Probability density function of the complex gain  $\bar{g}(t)$

Changing from Cartesian coordinates to polar coordinates ( $\bar{g} = g_r + \bar{g}_i = r \cdot e^{j\theta}$ ) by standard transformation yields the following joint probability density function in Equation 2.19.

$$p(r, \theta) = \frac{r}{2\pi \cdot \sigma_g^2} \cdot e^{\frac{-r^2}{2\sigma_g^2}} \quad (2.19)$$

$r$  and  $\theta$  are independent, where  $\theta$  has a uniform distribution, while the distribution of  $r$  is given in Equation 2.20 and is called the **Rayleigh distribution**.

$$p(|\bar{g}(t)|) = p(r) = \frac{r}{\sigma_g^2} \cdot e^{\frac{-r^2}{2\sigma_g^2}} \quad (2.20)$$

If such a type of fading is present with no path dominating among all received paths due to the absence of a line of sight, the amplitude of the received signal will vary according to a Rayleigh distribution. This form of fading is characterized by the absence of a line of sight component, which is a very strong and 'fast' path compared to all other paths. A plot of the distribution is given in Figure 2.6.

For determining the actual SNR at the receiver the instantaneous power has to be obtained rather than the instantaneous amplitude. This is given by the squared amplitude  $z = r^2 = |\bar{g}|^2$  and the distribution of  $z$  is given in Equation 2.21. In fact  $z$  has a  $\chi^2$  distribution with two degrees of freedom due to the two independent jointly Gaussian processes of the real and imaginary parts of the signal combining.

$$p(\bar{g}(t)^2) = p(z) = \frac{1}{2\sigma_g^2} \cdot e^{\frac{-z}{2\sigma_g^2}} \quad (2.21)$$

A plot of the distribution is given in Figure 2.7.

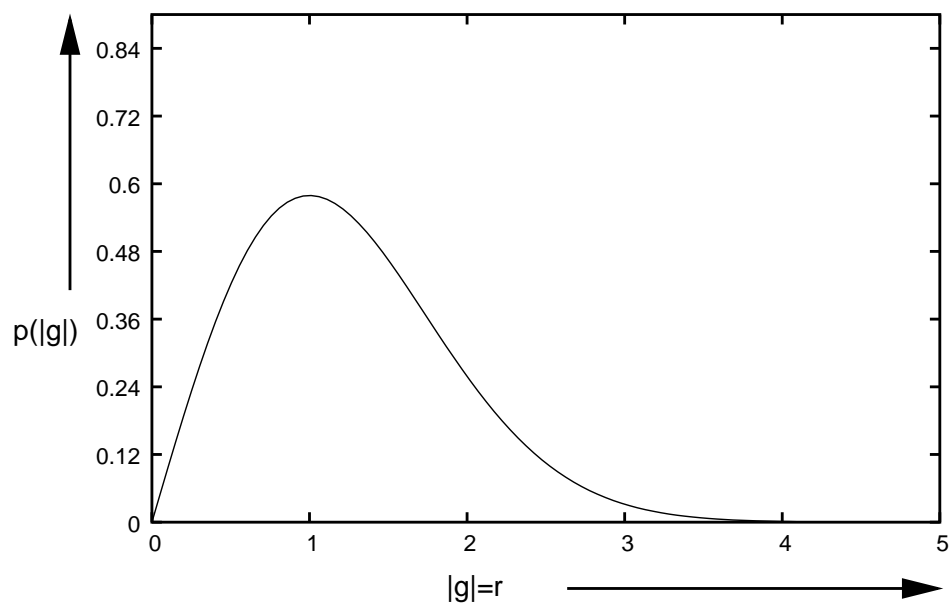


Figure 2.6: Probability density function of the magnitude of the complex gain  $|\bar{g}(t)|$ , which is Rayleigh distributed

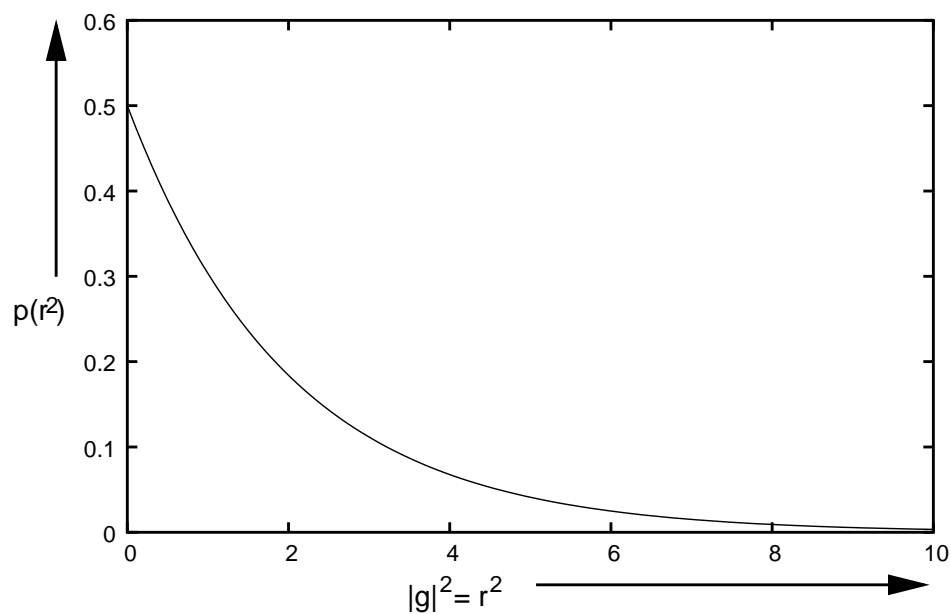


Figure 2.7: Probability density function of the squared magnitude of the complex gain  $|\bar{g}(t)|^2$ , which is  $\chi^2$ -distributed

From the cumulative distribution function and its asymptotic behavior (both not given here, refer to [4], page 46) two rules of thumb can be derived. First, the probability that the received instantaneous power will be 10 dB or more below the mean power level is 0.1. A 20 dB fade or more has the probability of 0.01 and so on. Second, the probability that the instantaneous power drops below a given level decreases only inversely with increasing the average power. Therefore doubling the power only reduces a level dropping probability by half.

In the case of an existing line of sight component, the distribution of  $r$  is no longer Rayleigh but **Rice**, since now one distinct path dominates, which means that it is received much stronger (in terms of power) than the remaining paths. Accordingly, the instantaneous power  $z$  resulting from the fading has a non central  $\chi^2$  distribution with two degrees of freedom. The Rice distribution depends on the ratio between power of the strong path and power of the remaining paths and can characterize therefore many different line-of-sight scenarios, while the Rayleigh distribution (only) characterizes the situation, when no path dominates, therefore a strict non-line-of-sight scenario. For a detailed derivation refer to [4].

For a small number of paths ( $< 5$ ), the assumption of the Gaussian process as a result of the central limit theorem does not fit adequately any more. In this case the amplitude  $r$  of the received signal can be assumed to have a **Nakagami distribution** density. The instantaneous power  $z$  of the signal has a  $\Gamma$  distribution. By varying a variable  $m$  the Nakagami distribution can take the absence or presence of a line of sight into account. In addition to this, the Nakagami distribution is more convenient for analytical work. For a detailed derivation and discussion refer to [4].

As already mentioned does the Rayleigh distribution show up in most non-line-of-sight settings, which are encountered mostly with indoor scenarios as well as with macrocells in urban areas. Rice distributions are encountered on the opposite with urban microcells and suburban macrocells (refer to [4]). However, by considering Rayleigh fading, one is working with the worst possible scenario, since in settings where the Rice distribution applies, fading is less destructive and the performance of communication systems is better.

The Nakagami distribution is an alternative distribution to the Rice distribution, it models line-of-sight scenarios, where a certain dominating path exists. Note that both distributions, the Nakagami as well as the Rice one, can be reduced to the Rayleigh distribution by setting the ratio between power of the dominating path and remaining power to zero

### 2.3.5 Second Order Statistics

In the previous Section the complex gain  $\bar{g}(t)$  as well as the complex transfer function  $\bar{G}(f)$  were shown to be Gaussian random processes in time, respectively in frequency. In order to describe a Gaussian random process it is sufficient to know its mean and its autocorrelation function or the transform of it, the **power spectrum**. The mean has already been shown implicitly in the previous Section. In this Section we desire to obtain the second order description of the process in the case of Doppler spread as well as in the case of delay spread. At first the second order statistics in the case of Doppler spread are derived, afterwards we derive them for the case of delay spread.

In the presence of Doppler spread only, thus  $s(t - \tau_i) \approx s(t)$ , the received signal  $\bar{y}(t)$  is given by the product of the transmitted signal  $\bar{s}(t)$  and the complex gain of the channel  $\bar{g}(t)$ .

$\bar{g}(t)$  is time variant and is given by Equation 2.10. If the input signal is a tone at the carrier frequency, therefore  $\bar{s}(t) = 1$  for example, the received signal consists of multiple tones at frequencies in the vicinity of the carrier with a maximum shift of the Doppler frequency  $f_d$ . Hence the tone is spread.

We desire the power spectrum of such a reception. Considering a mobile receiver moving with the speed  $v$  in a multipath environment as shown in Figure 2.4 each Doppler shift frequency  $\nu$  is given by Equation 2.22 .

$$\nu = f_d \cdot \cos(\gamma) \quad (2.22)$$

In general  $\nu$  varies from  $+f_d$ , resulting from reflected paths in front of the receiver, to  $-f_d$ , resulting from reflected paths behind the receiver (behind and in front relate to the direction of movement of the receiver). Since  $\cos(\cdot)$  is an even function, the Doppler shift frequency  $\nu$  might result from a scatterer at the left or the right side of the receiver, therefore from a scattering angle of  $+\gamma$  or  $-\gamma$ . Differentiating Equation 2.22 yields us the relationship between (small) ranges of  $\nu$  and of the angle  $\gamma$  in Equation 2.23.

$$\frac{d\nu}{d\gamma} = f_d \cdot \sin(\gamma) = f_d \cdot \sqrt{1 - \cos(\gamma)^2} = f_d \cdot \sqrt{1 - \left(\frac{\nu}{f_d}\right)^2} \quad (2.23)$$

Assume that the amount of scatterers is high, therefore the power received from differential angle  $d\gamma$  is given by the product of power density  $P(\gamma)$  and differential angle  $d\gamma$ . With this we can relate the received power  $S_{\bar{g}}$  to the Doppler shift frequency  $\nu$  in Equation 2.24 and therefore receive the **power spectrum**  $S_{\bar{g}}(\nu)$ .

$$S_{\bar{g}}(\nu) = \frac{P(\gamma) + P(-\gamma)}{f_d \cdot \sqrt{1 - \left(\frac{\nu}{f_d}\right)^2}} \quad (2.24)$$

Now consider the special case of **isotropic scattering**, which implies that the power received from different angles is equivalent ( $P(\gamma) = \frac{(\sigma_{\bar{g}})^2}{2\pi}$ ). In this special case Equation 2.24 turns into Equation 2.25.

$$S_{\bar{g}}(\nu) = \frac{(\sigma_{\bar{g}})^2}{\pi \cdot f_d} \cdot \frac{1}{\sqrt{1 - \left(\frac{\nu}{f_d}\right)^2}} \quad (2.25)$$

Equation 2.25 describes an U shaped spectrum, shown in Figure 2.8. It is often referred to as **Jakes** power spectrum [8].

From the power spectrum, the autocorrelation function of the complex gain is easy to derive by inverse Fourier transform, which yields Equation 2.26.

$$\begin{aligned} r_{\bar{g}}(\tau) &= \int_{-f_d}^{f_d} S_{\bar{g}}(\nu) \cdot e^{2\pi j \cdot \nu \cdot \tau} d\nu = \frac{\sigma_{\bar{g}}^2}{2\pi} \cdot \int_{-\pi}^{\pi} e^{2\pi j \cdot f_d \cdot \cos(\gamma) \cdot \tau} d\gamma \\ &= \sigma_{\bar{g}}^2 J_0(2\pi f_d \tau) = \sigma_{\bar{g}}^2 J_0\left(2\pi \frac{x}{\lambda}\right) \end{aligned} \quad (2.26)$$

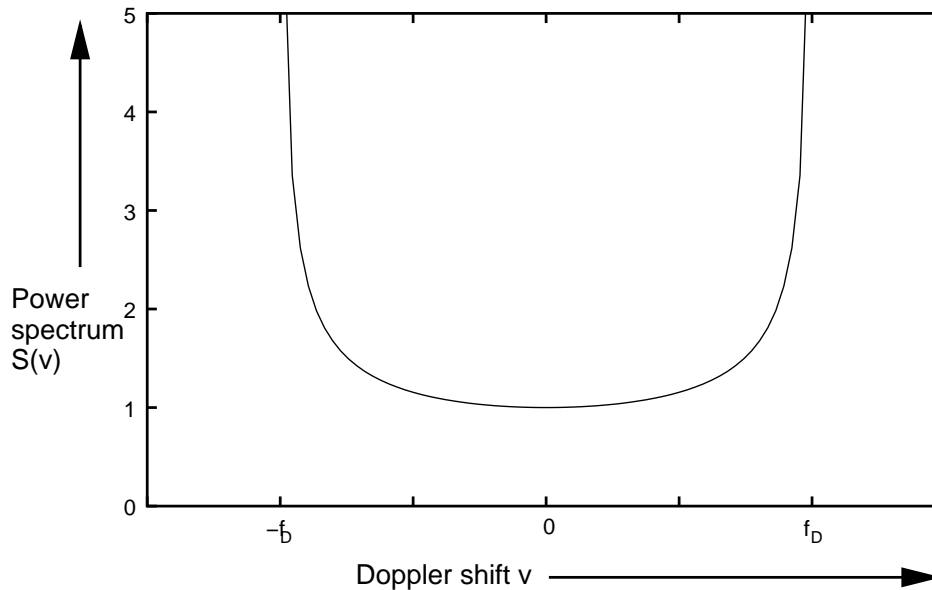


Figure 2.8: Power spectrum for the isotropic scattering case

Equation 2.26 relates the autocorrelation function depending on a time difference  $\tau$  with a space difference  $x$ . The fact that the autocorrelation function only depends on differences, either in time or in space, result from the assumption that  $\bar{g}(t)$  is a wide sense stationary Gaussian random process. For wide sense stationary processes Equation 2.27 is valid.

$$E[\bar{g}(t)\bar{g}^*(t-\tau)] = r_{\bar{g}}(\tau) \quad (2.27)$$

Under the assumption, that the scatterers at different Doppler shifts  $\nu$  are uncorrelated,  $\bar{g}(t)$  is in fact uncorrelated (shown by setting  $\bar{g}(t)$  from Equation 2.10 in the left side of Equation 2.27). This assumption is called the **wide sense stationary (WSS) assumption**.

From the autocorrelation function of the complex gain in Equation 2.26 a measure in time can be derived characterizing the channel encountered. This is called the **coherence time** and indicates the time span the channel roughly stays constant. One mathematical definition of the coherence time is given in Equation 2.28, which equals an autocorrelation value of 0.98 [4]. However, this definition is somewhat subjective and other definitions might be found in [12, 13, 17].

$$T_c = \frac{1}{2\pi \cdot \nu_{rms}} = \frac{1}{\sqrt{2}\pi f_d} \quad (2.28)$$

In Equation 2.28  $\nu_{rms}$  denotes the standard deviation of the Doppler power spectrum  $S_{\bar{g}}(\nu)$  given by Equation 2.24. For the isotropic scattering case the variance is  $\nu_{rms} = \frac{f_d}{\sqrt{2}}$ . In Table 2.9 typical values for the coherence time are shown. Note that these values only depend on the carrier frequency used. Therefore if a wireless local area network according to IEEE 802.11b is installed, the system can assume a coherence time of 28.1 ms if all objects within the relevant area do not move faster than  $1 \frac{m}{s}$ . However, if the system is installed

Carrier Frequency	$T_c$ @ $1\frac{m}{s}$	$T_c$ @ $10\frac{m}{s}$	$T_c$ @ $20\frac{m}{s}$	$T_c$ @ $100\frac{m}{s}$
1 Mhz	68.2 s	6.82 s	3.41 s	0.68 s
100 Mhz	0.68 s	68.2 ms	34.1 ms	6.82 ms
1 Ghz	68.2 ms	6.82 ms	3.41 ms	0.68 ms
2.4 Ghz	28.1 ms	2.81 ms	1.4 ms	0.28 ms
5.4 Ghz	12.5 ms	1.25 ms	0.62 ms	0.12 ms
10 Ghz	6.82 ms	0.68 ms	0.34 ms	68.2 $\mu$ s
60 Ghz	1.12 ms	0.11 ms	56.2 $\mu$ s	11.2 $\mu$ s

Table 2.9: Coherence time values for different carrier frequencies at speeds comparable to walking ( $1\frac{m}{s}$ ), a slow car ( $10\frac{m}{s}$ ), a fast car ( $20\frac{m}{s}$ ) and traveling per train (ICE  $100\frac{m}{s}$ )

near a highway, the coherence time is significantly smaller. The required bandwidth has no impact, as long as it is much smaller than the carrier frequency. If the required bandwidth is not significantly smaller compared to the carrier frequency, the coherence time to be expected equals the coherence time of the highest frequency involved in the communication scheme.

At next we are interested in the second order statistics stemming from the delay spread only. As we have seen, it was possible to obtain a power density distribution in the frequency domain, characterizing the Doppler spread in an isotropic environment. From this the autocorrelation in the time domain was derived, indicating the second order statistical behavior in time of the complex gain function  $\bar{g}(t)$ . As it was already shown in Section 2.3.3 the Doppler spread gives a wireless channel a time selective behavior, however the severity of this behavior depends on the time structure of the transmitted signal. In contrast does the delay spread give a wireless channel a frequency selective behavior. Therefore we desire now an autocorrelation function in frequency, which yields us the second order statistical behavior of the complex transfer function  $\bar{G}(f)$  from Equation 2.13.

In the presence of delay spread only the wireless channel can be modelled as linear time invariant filter. Thus the received signal  $\bar{y}(t)$  is given by the convolution of the transmitted signal  $\bar{s}(t)$  and the channel impulse response  $\bar{g}(t)$ , given by Equation 2.12. Accordingly, the received signal in the frequency domain is given by the product of the frequency domain representation of the transmitted signal and the transfer function  $\bar{G}(f)$  of the channel, given by Equation 2.13. We are interested in a spaced frequency correlation function of  $\bar{G}(f)$ , that is a function which gives us the correlation between the transfer function at different frequencies. If two tones at different frequencies are transmitted, the desired correlation function gives us the correlation between the received signals of the two tones. In general this function is given by Equation 2.29.

$$\bar{r}_{\bar{G}}(f, f - \Delta f) = \frac{1}{2} \cdot E [\bar{G}(f) \cdot \bar{G}^*(f - \Delta f)] \quad (2.29)$$

Substitution of Equation 2.13 into Equation 2.29 yields Equation 2.30.

$$\bar{r}_{\bar{G}}(f, f - \Delta f) = \frac{1}{2} \cdot E \left[ \sum_{\forall i} \sum_{\forall k} \bar{A}_i \bar{A}_k^* \cdot e^{-2\pi j \cdot f \cdot (\tau_i - \tau_k)} \cdot e^{-2\pi j \Delta f \cdot \tau_k} \right] \quad (2.30)$$

If scatterers at different delays are uncorrelated, this autocorrelation function depends only on the frequency difference  $\Delta f$ , due to the then existing relationship given by Equation 2.31. This assumption is called the **uncorrelated scatterers (US) assumption** of wireless channels.

$$\frac{1}{2}E \left[ \sum_{\forall i} \sum_{\forall k} \bar{A}_i \bar{A}_k^* \right] = \frac{1}{2}E \left[ \sum_{\forall k_i} \bar{A}_i \bar{A}_{k_i}^* \right] = \sigma_i \quad (2.31)$$

Here  $k_i$  indicates all scatterers with the same delay  $\tau_i$ . With this Equation 2.30 turns into Equation 2.32.

$$\bar{r}_{\bar{G}}(\Delta f) = \sum_{\forall k} (\sigma_k)^2 \cdot e^{-2\pi j \Delta f \cdot \tau_k} \quad (2.32)$$

Now consider many scatterers to be present. In this case the summation in Equation 2.32 becomes a density depending on the delay  $\tau$ . This density is called the **power delay profile**  $P(\tau)$  and with this we obtain Equation 2.33.

$$\bar{r}_{\bar{G}}(\Delta f) = \int_0^{\infty} P(\tau) \cdot e^{-2\pi j \Delta f \cdot \tau} \cdot d\tau \quad (2.33)$$

For the power delay profile one idealized but often used function is the exponential profile given by Equation 2.34.

$$P(\tau) = \frac{(\sigma_{\bar{g}})^2}{\tau_{rms}} \cdot e^{-\frac{\tau}{\tau_{rms}}} \quad (2.34)$$

$(\tau_{rms})^2$  is the delay variance (mean squared delay) given by Equation 2.35. The square root of this, the standard deviation of the delay, is an often used measure for the delay spread of a propagation environment (also used in Table 2.7).

$$\tau_{rms}^2 = \frac{1}{\sigma_{\bar{g}}^2} \cdot \int_0^{\infty} (\tau - \tau_m)^2 \cdot P(\tau) d\tau \quad (2.35)$$

$\tau_m$  denotes the mean delay and is given by Equation 2.36.

$$\tau_m = \frac{1}{\sigma_{\bar{g}}^2} \cdot \int_0^{\infty} \tau \cdot P(\tau) d\tau \quad (2.36)$$

For the exponential power delay profile  $\tau_{rms}$  equals  $\tau_m$ .

From the autocorrelation function of the transfer function of the wireless channel with uncorrelated scatterers a measure in frequency can be derived characterizing the channel encountered. The meaning of this measure is related to the coherence time and is called the **coherence bandwidth**. The coherence bandwidth measures roughly the frequency spacing for which the channel does not change significantly. Again the exact mathematical definition is to some extent subjective. One definition of the coherence bandwidth is given by Equation 2.37, following [4]. Other definition might be found in [12, 13, 17].

$$W_c = \frac{1}{2\pi\tau_{rms}} \quad (2.37)$$

Environment	$W_c$
Urban	6.4 kHz - 160 kHz
Suburban	80 kHz - 800 kHz
Indoor	0.64 MHz - 6.4 MHz

Table 2.10: Coherence bandwidth ranges for three typical environments

In Table 2.10 ranges of the coherence bandwidth are given for different environments. Note that the carrier frequency has no influence on the coherence bandwidth, therefore if one happens to be in an indoor environment, one will always encounter a coherence bandwidth of some MHz, no matter if for example a wireless local area network working at 2.4 GHz is used or at a carrier frequency of 5.4 GHz. If the coherence bandwidth is much smaller than the required bandwidth for transmission, the system will suffer from ISI, no matter at which carrier frequency the system is working. Therefore, as the Table highlights, it is much easier to communicate at high data rates in indoor scenarios due to the large coherence bandwidth than in urban environments, here ISI degrades the performance severely.

Up to now, we have only investigated the second order statistics in the presence of one phenomenon. In the case of the time selective behavior of the complex gain function  $\bar{g}(t)$  caused by Doppler spread we obtained a gain autocorrelation function in time and as Fourier transform the Doppler power spectrum in the frequency domain. In the case of the frequency selective behavior of the transfer function  $\bar{G}(f)$  caused by delay spread we obtained a gain autocorrelation function in the frequency domain and as Fourier transform the power delay profile in the time domain.

At next we focus on the presence of both effects at the same time and will obtain some results regarding the correlation behavior in both domains.

First let us recall the input output relationship in the case of many scatterers given by Equation 2.9.

$$\bar{y}(t) = \int_0^\infty \int_{-f_d}^{f_d} \bar{\rho}(\nu, \tau) \cdot e^{2\pi j \cdot \nu \cdot t} \cdot \bar{s}(t - \tau) \cdot d\nu d\tau$$

$\bar{\rho}(\nu, \tau)$  is the delay-Doppler spread function from Equation 2.8. Observing the output in the case of a single carrier input at frequency  $f$ , where  $s(t) = e^{2\pi j \cdot f \cdot t}$ , we obtain the output given in Equation 2.38.

$$\bar{y}(t) = \int_0^\infty \int_{-f_d}^{f_d} \bar{\rho}(\nu, \tau) \cdot e^{2\pi j \cdot \nu \cdot t} \cdot \bar{e}^{2\pi j \cdot f \cdot t} \cdot e^{-2\pi j \cdot f \cdot \tau} \cdot d\nu d\tau = e^{2\pi j \cdot f \cdot t} \cdot \bar{G}(t, f) \quad (2.38)$$

Here  $\bar{G}(t, f)$  is the time variant transfer function and determines the complex gain experienced at frequency  $f$  at time  $t$ . It was already introduced in Equation 2.16. Since both, delay and Doppler spread are now present, we desire a time-frequency correlation function of  $\bar{G}(t, f)$ . That is, a function representing the correlation between the complex gain at time  $t$  and at frequency  $f$ , compared to the complex gain at time  $t + \Delta t$  and at frequency  $f + \Delta f$ .

Considering the WSS assumption (scatterers at different Doppler shifts are uncorrelated) and the US assumption (scatterers at different delays are uncorrelated), this desired function becomes the one in Equation 2.39, only depending on the delay and frequency differences present.

$$r_{\bar{G}}(\Delta t, \Delta f) = \int_{-\infty}^{\infty} \int_{-\infty}^{\infty} S_{\bar{g}}(\nu, \tau) \cdot e^{2\pi j \nu \Delta t} \cdot e^{2\pi j \Delta f \tau} d\nu d\tau \quad (2.39)$$

In this equation  $S_{\bar{g}}(\nu, \tau)$  is called the **delay-Doppler power density function** or also the **scattering function**. It represents the power density of the environment at Doppler shift  $\nu$  and delay  $\tau$ . This function is related to the delay power profile introduced in Equation 2.33 by Equation 2.40.

$$P(\tau) = \int_{-\infty}^{\infty} S_{\bar{g}}(\nu, \tau) d\nu \quad (2.40)$$

It is related to the Doppler spectrum in a similar way by integrating the scattering function in the delay domain.

In order to determine the functional behavior of the scattering function let us assume that the Doppler spectrum is not linked to the delay profile. Then the scattering function is called to be **separable**. Therefore the scattering function is given by Equation 2.41.

$$S_{\bar{g}}(\nu, \tau) = \frac{S_{\bar{g}}(\nu) \cdot P(\tau)}{\sigma_{\bar{g}}^2} \quad (2.41)$$

With this assumption the autocorrelation function from Equation 2.39 becomes simpler and is given in Equation 2.42.

$$r_{\bar{G}}(\Delta t, \Delta f) = \frac{r_{\bar{g}}(\Delta t) \cdot r_{\bar{G}}(\Delta f)}{\sigma_{\bar{g}}^2} \quad (2.42)$$

A plot of the scattering function is given in Figure 2.9, where the power spectrum is Jakes like and the power delay profile has an exponential behavior.

### 2.3.6 Fading Rate and Duration

In Section 2.3.4 a rule of thumb was given, indicating the probability of a fade on a wireless channel by 10 dB, 20 dB and so on. As we have seen from the discussion of the complex gain of a time invariant channel, at some instances the channels attenuation might exceed a certain threshold. Clearly, this depends on the time variant behavior of the channel and therefore ultimately on the velocity assumed to be present in the propagation environment.

Given a certain attenuation threshold  $X$  it is of great interest for system design to know the average rate with which the complex gains amplitude  $r(t) = |\bar{g}(t)|$  will cross this rate. This rate is called the **fading rate**. In addition it is of interest to know the average duration the complex gains amplitude will be below the threshold  $X$ , which is called the **fading duration**.

Here we will derive both averages and will start with the fading rate. For the derivation consider first the sketch of a level crossing given in Figure 2.10. Here the complex gains amplitude is a time  $t_i$  below the given threshold, a time  $t_i + dt$  it is above the threshold.

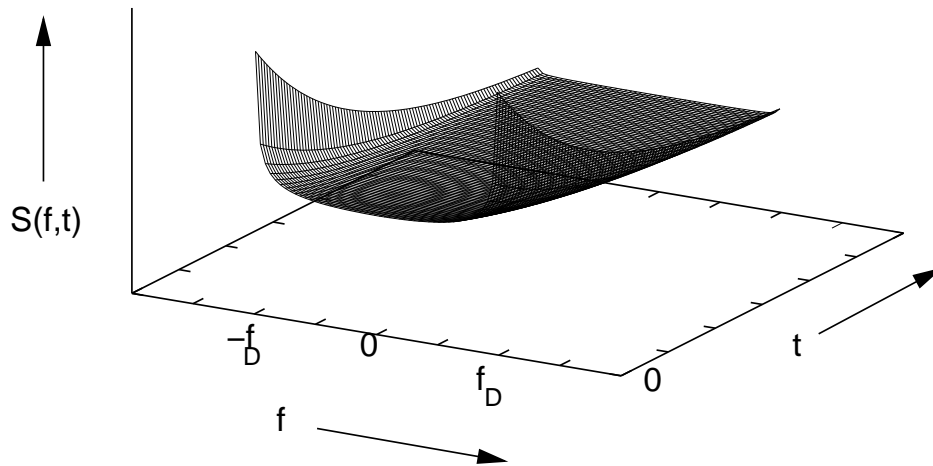


Figure 2.9: Scattering function in the case of seperability

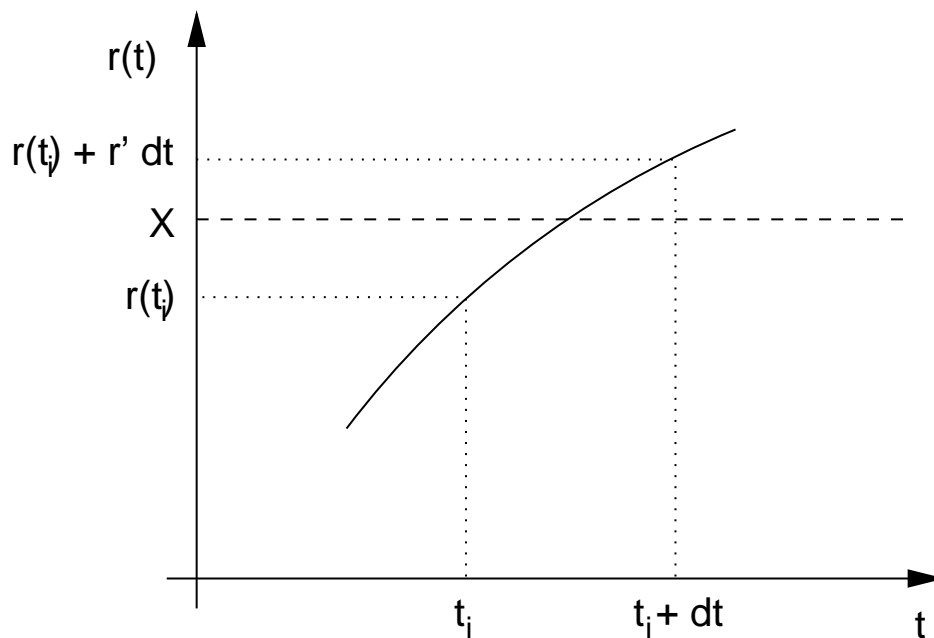


Figure 2.10: Illustration of a level crossing at a threshold of  $X$

A level crossing will take place, if the differential increase of the complex gains amplitude during the duration  $dt$  is larger or equal to  $X - r(t)$ , therefore if  $X - r(t) \leq dr = r' \cdot dt$  which equals  $X - r' \cdot dt \leq r(t) < X$  (we only focus on upward crossings, since these will yield the desired overall crossing rate, therefore assume in general here  $r' > 0$ ). The probability of such an increase of  $r(t)$  at time  $t$  during the interval  $dt$  at a slope  $r'$  with a slope increase of  $dr'$  is given by Equation 2.43.

$$dr' \int_{X-r' \cdot dt}^X p_{r,r'}(r, r') dr \quad (2.43)$$

With this we easily obtain the overall probability of an upward crossing in Equation 2.44.

$$P_{up} = \int_0^\infty \int_{X-r' \cdot dt}^X p_{r,r'}(r, r') dr dr' = dt \cdot \int_0^\infty r' p_{X,r'}(r, r') dr' \quad (2.44)$$

The second integrand in this equation is the expected number of upward level crossings in any  $dt$ , thus this yields the fading rate as explicitly shown in Equation 2.45.

$$R_f(X) = \int_0^\infty r' p_{X,r'}(r, r') dr' \quad (2.45)$$

For Rayleigh fading channels, the joint probability of the complex gains amplitude and derivative of it is given by Equation 2.46.

$$p_{r,r'}(r, r') = \frac{r}{\sqrt{2\pi} \cdot \sigma_g \cdot \sigma_{g'}} e^{-\frac{1}{2} \cdot \left( \frac{r^2}{\sigma_g^2} + \frac{r'^2}{\sigma_{g'}^2} \right)} \quad (2.46)$$

Substitution of Equation 2.46 into Equation 2.45 yields, under the assumption of isotropic scatterers, Equation 2.47 (for more refer to [4]).

$$R_f(X) = \sqrt{2\pi} \cdot f_d \cdot \frac{X}{\sqrt{2\sigma_g^2}} \cdot e^{-\frac{X}{\sqrt{2\sigma_g^2}}^2} \quad (2.47)$$

In Table 2.11 we give some values of the fading rates for a 10 dB fade for various carrier frequencies and different velocities of the receiver.

From Equation 2.45 it is easy to derive the fading duration. Consider the relationship given by Equation 2.48.

$$P(r \leq X) = R_f(X) \cdot T_f(X) \quad (2.48)$$

Once the fading rate is given, the fading duration denoted by  $T_f(X)$  can be derived by considering the overall probability that the complex gains amplitude is below the given threshold. For a Rayleigh fading channel we therefore obtain together with the CDF of the complex gains amplitude (not given in this report, refer to [4]) Equation 2.49 for the fading duration. Note that this again assumes isotropic scattering.

Carrier Frequency	$R_f(0.1)$ @ $1\frac{m}{s}$	$R_f(0.1)$ @ $10\frac{m}{s}$	$R_f(0.1)$ @ $20\frac{m}{s}$	$R_f(0.1)$ @ $100\frac{m}{s}$
1 Mhz	0.0005 Hz	0.0054 Hz	0.0119 Hz	0.0594 Hz
100 Mhz	0.059 Hz	0.594 Hz	1.19 Hz	5.94 Hz
1 Ghz	0.59 Hz	5.94 Hz	11.9 Hz	59.4 Hz
2.4 Ghz	1.41 Hz	14.1 Hz	28.2 Hz	141 Hz
5.4 Ghz	3.17 Hz	31.6 Hz	63.3 Hz	317 Hz
10 Ghz	5.94 Hz	59.4 Hz	119 Hz	594 Hz
60 Ghz	35.2 Hz	352 Hz	704 Hz	3.52 kHz

Table 2.11: Fading rates for a fading threshold of 10 dB equaling  $X = 0.1$  for different carrier frequencies at velocities comparable to walking ( $1\frac{m}{s}$ ), a slow car ( $10\frac{m}{s}$ ), a fast car ( $20\frac{m}{s}$ ) and traveling per train (ICE  $100\frac{m}{s}$ )

Carrier Frequency	$T_f(0.1)$ @ $1\frac{m}{s}$	$T_f(0.1)$ @ $10\frac{m}{s}$	$T_f(0.1)$ @ $20\frac{m}{s}$	$T_f(0.1)$ @ $100\frac{m}{s}$
1 Mhz	8.4 s	800 ms	400 ms	80 ms
100 Mhz	84 ms	8 ms	4 ms	$800\mu$ s
1 Ghz	8.4 ms	0.8 ms	0.4 ms	$80\mu$ s
2.4 Ghz	3.5 ms	0.3 ms	0.17 ms	$30\mu$ s
5.4 Ghz	1.6 ms	0.16 ms	$80\mu$ s	$16\mu$ s
10 Ghz	0.84 ms	$84\mu$ s	$42\mu$ s	$8.4\mu$ s
60 Ghz	0.142 ms	$14.2\mu$ s	$7.6\mu$ s	$1.42\mu$ s

Table 2.12: Fading duration for a fading threshold of 10 dB equaling  $X = 0.1$  for different carrier frequencies at velocities comparable to walking ( $1\frac{m}{s}$ ), a slow car ( $10\frac{m}{s}$ ), a fast car ( $20\frac{m}{s}$ ) and traveling per train (ICE  $100\frac{m}{s}$ )

$$T_f(X) = \frac{1 - e^{-\frac{X}{\sqrt{2\sigma_g^2}}^2}}{\sqrt{2\pi} \cdot f_d \cdot \frac{X}{\sqrt{2\sigma_g^2}} \cdot e^{-\frac{X}{\sqrt{2\sigma_g^2}}^2}} = \frac{1 - e^{-\frac{X}{\sqrt{2\sigma_g^2}}^2}}{R_f(X)} \quad (2.49)$$

In Table 2.12 we give the corresponding fading durations for a threshold of  $X = 0.1$

From the asymptotic behavior of the fading rate as well as the fading duration with respect to a varying fading threshold, one further rule of thumb can be derived. If the fading threshold is reduced by a factor of 4, which equals a decrease of 6 dB, then the fades are on the average half as long while they occur half as frequent. Therefore increasing the transmission power by a factor of 4 yields exactly this result on the fading rate and duration.

## Chapter 3

# Modulation Channel

While the effects of the radio channel have an attenuating impact on the relationship between transmitted and received signal, the modulation channel has an additive impact on this relationship. Two major sources of effects are modelled in general. The first one is **noise**. Noise is always of stochastic nature and varies with time. It is denoted by  $n(t)$ .

The second effect corrupting the received signal in an additive manner is **interference**. Interference is caused by other RF transmitting electronic devices. As it is with the noise, interference has a stochastic nature and varies with time. It is denoted by  $j(t)$ . Interference is due to other systems operating in the same frequency band in the case of unlicensed bands, or to co- and adjacent-channel interference in licensed bands. **Co-channel interference** happens due to frequency re-utilisation in a cellular environment and is unavoidable. **Adjacent channel interference** is due to realistic filters letting some power be transmitted in the sidebands. Interference is always the results of other wireless systems operating in the same or nearby frequencies.

The quality of demodulation and decoding of a signal depends on the difference between the power of the received signal and the power of other signals with power in the same frequency band — interference — added to the power of the noise.

### 3.1 Noise

Noise is always present and comes from several sources, e. g. atmospheric disturbances, electronic circuitry, human-made machinery. The first two belong to the group of thermal noise sources described in 3.1.1. Noise produced by human-made sources is described in more detail in Section 3.1.3.

#### 3.1.1 Thermal Noise

Thermal noise is due to the movement of charged particles inside electronic components existent in every receiver system and is therefore unavoidable. The characteristics of thermal noise were firstly studied for a resistor. Since many other noise sources besides resistors are Gaussian and have a spectrum which is constant over a wide frequency range, the calculation of the noise power produced by a thermal noise source is shown here on the example of a resistor.

The voltage at the terminals of a resistor is Gaussian-distributed and with variance proportional to the temperature at which the resistor operates. A simplified expression for the spectral density of thermal noise from a resistor of resistance  $R$  is given by

$$G_{v_n}(f) \approx 2 \cdot k \cdot \mathcal{T} \left( 1 - \frac{h \cdot |f|}{2 \cdot h \cdot \mathcal{T}} \right) |f| \ll \frac{k\mathcal{T}}{h},$$

where  $f$  is the frequency,  $h = 6.62 \cdot 10^{-34} \text{ J} \cdot \text{s}$  the Planck constant,  $k = 1.37 \cdot 10^{-23} \text{ J/deg}$  the Boltzman constant and  $\mathcal{T}$  the absolute temperature ([3]). This expression can be further simplified since for usual working temperatures,  $\frac{h \cdot |f|}{2 \cdot h \cdot \mathcal{T}} \ll 1$  and the spectrum of the noise can be considered constant over the frequencies used:  $G_v(f) \approx 2 \cdot k \cdot \mathcal{T}$ . Take for example a working temperature of  $0^\circ$ , and the condition for the approximation becomes  $f \ll 22 \cdot 10^{-12}$ , and the VHF and UHF frequency bands are way within the limits for which the approximation is valid.

The power of thermal noise can be obtained using the maximum power transfer theorem:

$$G_n = 1/2 \cdot k \cdot \mathcal{T} [\text{W/Hz}] \tag{3.1}$$

Notice that the power delivered by a resistor at temperature  $\mathcal{T}$  is independent of the value of the resistance. Usually a temperature of  $\mathcal{T}_0 = 290^\circ$  is used as a reference for measurements and calculations.

This kind of noise is called white because it contains all frequencies, in analogy to white light, which contains all light frequencies. White noise is uncorrelated.

Thermal noise sources have a power spectral density which depends on the working temperature. There are also noise sources whose produced noise does not depend on the temperature. Nevertheless, an **effective noise temperature** is defined for every gaussian noise source, e. g. amplifiers, and is used in equation (3.1) to calculate the noise power introduced by the component on the system (see Appendix A of [3] for more details). This noise is always referred to the input of the component, so that it will also be filtered, as explained in the next section.

### 3.1.2 Filtered White Gaussian Noise

In practical systems of limited bandwidth, the noise is also filtered and is at the output no longer white, taking the shape of the filter's transfer function and no longer having all frequencies in the same proportion. This means that the noise becomes correlated when it is low-pass filtered. If an ideal low-pass filter of bandwidth  $B$  is assumed, the autocorrelation function of the coloured noise will be  $R_n(\tau) = 2 \cdot G_n \cdot \text{sinc}(2 \cdot B \cdot \tau)$ , where  $G_n$  is calculated as stated at the end of last section.

The **noise equivalent bandwidth** of a filter  $B_n$  is defined as the bandwidth of the ideal bandpass filter which would let the same gaussian white noise power through as the filter in question<sup>1</sup>. The average noise power at the output of the filter can then be expressed as  $N = g \cdot 2 \cdot G_n \cdot B_n$ , where  $g$  is the power gain of the filter at the centre frequency. If the noise has zero mean value, then  $\sigma_n = N$ .

---

<sup>1</sup>Note that every electronic component is, in this context, a filter.

The effective noise temperature and noise equivalent bandwidth can be found in the datasheets of electronic components. In mobile communication systems these values are usually not relevant since the limitations to system performance are due to interference and man-made noise (see Section 3.2), which takes values several magnitudes higher.

### 3.1.3 Man-made Noise

Man-made noise is noise produced by machines operated by humans. It is noise because it is energy radiated by machines which are not supposed to generate that energy. Their main purpose is some other function, but due to turning on and off of electrical and electronic components or to wiring, they radiate electromagnetic energy which can disturb wireless communications nearby.

The characterisation of man-made noise is very complicated, since many parameters have to be measured and they are always specific to the measurement environment. The parameters to be measured include average total power, power spectrum, probability distribution of the noise voltage, the pulse heights, widths and rates, as well as system specific parameters like dependence on antenna polarisation, height and directivity, and long-time dependence on time and location. In [5] three methods for measuring man-made noise are explained. Also some measurement results are presented, which lead to the conclusion that for frequencies above 4 GHz the power of man-made noise is negligible compared to the noise produced by a typical receiver. Nevertheless, these results were obtained in the 70's, and it must be taken in consideration that due to the technological advances in the last decades typical receivers nowadays probably have much lower noise figures than 30 years ago.

### 3.1.4 Some Results

Quite few results exist about man-made noise, but some are presented in the following paragraphs.

In [2] some results of measurements in indoor environment are documented, which were made with the objective of developing empirical impulsive noise models. The measurements were made with a 40 MHz bandwidth receiver at 918 MHz, 2.44 GHz and 4 GHz in different indoor environments: a department store, a grocery store, soft-partitioned office buildings and a hard-partitioned office building. It could be concluded that the main noise sources of impulsive noise are microwave ovens, photocopiers, printers, elevator door switched and ignition systems. Measurement results show that the noise from a microwave oven (1st order statistics) can be modelled by a 2.45 GHz carrier modulated by a pulse train at the AC power frequency. Some conclusions can be taken from the measurement results:

- amplitude of power of noise pulses is greater in the 918 MHz band than in the others (see Table 3.1);
- amplitudes of the power of the impulses are not gaussian distributed;
- noise pulse durations were similar in all the measured frequency bands and the average values lie between 120 ns and 150 ns;
- for statistics on the rate of the pulses, refer to [2].

Frequency	Average Amplitude	$\sigma$	1% Probability	0.001% Probability
914 MHz	18.87	6.86	40	63
2.44 GHz	16.14	6.99	29	45
4 GHz	11.75	5.87	23	43

Table 3.1: Statistics of the peak power of the noise pulses measured at the 2 first locations; amplitude power was measured above thermal noise  $k \cdot T_0$ . All values in dB. (source [2]).

- data relative to the impulsive noise generated by the photocopier, the microwave oven and the elevator door switched can also be found in [2].

In [1] some are presented for man-made noise due mainly to cars (ignition and motors). The distribution of the power is also not gaussian, but follows a combination of a gaussian with a Weibull distribution.

Most man-made noise measurement results available are 3 decades old, as well as the models derived from them. Measurements reported in [6] indicate that those results are no longer valid, due to the technological advances on the one hand, which have improved the isolation of noise sources, and to the changes in the way of life on the other, where a personal computer, a television and cordless phones belong to almost every home. The new environments have new noise sources, whose characteristics need to be measured to develop new models. Nevertheless, the characteristics presented here provide a more realistic scenario than simply assuming uncorrelated or non-existing man-made noise.

## 3.2 Interference

In general the source of noise is a source which primarily does not intend to produce electromagnetic disturbance patterns, for example microwaves ovens or other electrical or electronic equipment. Another source of noise is given by the thermal effects existing for example in any electric circuit as in amplifiers.

Beside these sources of signal distortion, other communication system might be active in the environment. Such sources, which have the primary goal to produce electromagnetic radiation for communication purposes are not represented by noise, instead they are represented by interference. Like noise, interference has a additive distorting impact on the signal. For example, interference occurs in cellular systems, due to the fact that bandwidth is limited and system operators have to reuse certain spectra of the overall bandwidth. Frequency planning is one method to control interference in cellular systems. In unlicensed bands, interference may stem from local wireless networks, which just happen to be deployed quite close to each other. In general there are different kinds of interference with a different impact on the received signal.

First their is co-channel interference [4]. Co-channel interference occurs if two transmission devices operating within the same radio frequency band are active and a receiver, originally trying to receive the signal from one transmitter also receives a (weak) signal from the second transmitter. In cellular systems co-channel interference is an important factor limiting the systems performance, more important than noise (see [4], page 8). If more than two or three interference sources are active, interference may be modelled as white Gaussian

process, adopting many of the characteristics discussed in the previous Section about noise. The average interference power is then derived from the path loss equations of Section 2.1.

In unlicensed bands co-channel interference is also an important issue to take into consideration. Here, the same assumption may be made as with a cellular system: if multiple interference sources exist, the interference can be modelled as white Gaussian noise, which changes the consideration of interference much easier. The interference power level can be determined by path loss equations then.

Beside co-channel interference there is also the possibility that transmissions conveyed on a different but close frequency band produce a significant interference power in a receiver. This is mainly due to imperfect pass band filters and is called adjacent channel interference ([13]). Adjacent channel interference is encountered in cellular systems as well as in unlicensed bands.

In the following we give a rough, example analysis for the severity of co-channel interference in cellular systems. Note that in principle the same derivation is valid for any situation where multiple transmitters operate within the same frequency band, just separated by a certain distance from each other and from the receiver, trying to detect the signal originally transmitted to him (as it is with transmissions in unlicensed bands).

Consider a cellular system where the cell radius is denoted by  $R$  and the separation of cells operating at the same frequency band is denoted by  $D$ . We consider a receiver which is located at the fringe of a cell, therefore the distance between the desired base station (transmitter) and it (receiver) is equal to  $R$ . If we denote by  $P_0$  the overall used transmission power of each base station, then following from the path loss equation the power level of the desired signal is given by Equation 3.2.

$$P_y = \frac{P_0}{R^k} \quad (3.2)$$

$k$  depends on the environment of this scenario, values where given in Section 2.1. Following Equation 3.2 the interfering power level received from each base station (interfering transmitters) of the neighboring cells is given by Equation 3.3.

$$P_j = \frac{P_0}{(D - R)^k} \quad (3.3)$$

Considering  $i$  equally strong interfering transmitters, each one at one of the neighboring cells (which is a pessimistic assumption) in this scenario (note that for a hexagonal cell layout,  $i = 6$ ), the ratio between desired signal power and interfering power level is given by Equation 3.4.

$$CIR = \frac{P_y}{i \cdot P_i} = \frac{1}{i} \cdot \left( \frac{D - R}{R} \right)^k \quad (3.4)$$

One important fact about co-channel interference in a cellular environment is that increasing the transmission power at each base station (so at each transmitter) provides no system improvement regarding the interference power level, since Equation 3.4 is independent of the transmitted power. For a further discussion on this refer to [4].

## Chapter 4

# Digital Channel

According to the mathematical model shown in Figure 1.2 in Chapter 1 the transmitted signal is influenced by three effects, which have been discussed in Chapter 2 and 3. For a digital communication system the question arises, how these signal distortions translate into noticeable service degradations of running applications. Common measures, indicating already the impact on higher communication layers, are for example the bit error rate (BER). It depends on the power ratio between received signal power and disturbing noise and interference power, as well as on the modulation used. Recalling the mathematical model of Chapter 1, the received signal is given by Equation 4.1.

$$y(t) = a(t) \cdot s(t) + n(t) + j(t) \quad (4.1)$$

A very common measure in order to characterize the instantaneous power ratio is the **Signal-to-Noise-and-Interference Ratio (SNIR)**, usually measured in dB. The SNIR is easily obtained from Equation 4.1 and is given in Equation 4.2.

$$\text{SNIR}(t) = \frac{a^2(t) \cdot s^2(t)}{2 \cdot (n^2(t) + j^2(t))} \quad (4.2)$$

In this Chapter the relationship between SNIR and SER is shown for an example modulation type. Note that there exist many different modulation types for which the derivations might significantly change. However, in principle the performance of all modulation types depends on the actual SNIR and therefore an example derivation will give a good insight to the nonlinear relationship between performance metrics of the modulation channel (SNIR) and performance metrics of the digital channel (SER or BER).

### 4.1 Structure of the Digital Channel

The received analog signal, which is subject to the phenomena described in the previous Chapters, is a sequence of analog pulses and has to be converted back into the digital bit sequence which originated it; this process is called demodulation. The demodulation can be separated into two phases: the demodulation itself, and the detection.

**Demodulator** The digitally modulated signal can be seen as a linear combination of functions which form an orthonormal base of a vector space. The function of the demodulator during each symbol period is to decompose the received waveform into a vector in that space. This vector contains the value of the projections of the received waveform into the functions in the orthonormal base of the vector space. This can be achieved either by a matched filter or a correlator [12], depending on the type of signal being demodulated. The vector is of dimension  $N$ , the same as the dimension of the transmitted signal.

**Detector** The detector's function is to compare the vector output from the demodulator with the values of the  $M$  possible waveforms. The distances in the vector space are compared, and the "closest" possible waveform is transmitted. The detection is made such that the probability of making a wrong decision is minimised.

The received signal is, thus, converted into a sequence of symbols (demodulation) and then into a sequence of bits (detection). This sequence of bits should be the same as the transmitted sequence of bits. This is not always the case, since errors occur. This error process can be described by an indicator sequence — a stream of '0' and '1' —, where a '1' represents wrongly received bits and a '0' correctly received ones. This conversion is possible provided that the amount of noise and interference at the receiver is known. In the following considerations the interference will not be taken into account, and SNR will be used instead of SNIR.

The steps for the conversion of the analog in the digital channel are illustrated in Figure 4.1. They consist of taking, for every bit time, the value of the received signal, dividing it by the sum of noise and interference in the same time period, and substituting them into the expression for the used modulation. The resulting bit error probability is then used to randomly generate the fate of a bit. The digital channel can thus be derived from the analog channel, by calculating with which probability a pulse received with a certain power can be correctly demodulated. Notice that, for a given analog channel, different digital channels can be generated, depending on the modulation used (second step in Figure 4.1).

The calculation of the probability of correctly demodulating a symbol is shown using the examples of binary pulse amplitude modulation (PAM) over AWGN channel and over a Rayleigh fading channel in Sections 4.2 and 4.3, respectively. In Section 4.4 results for most commonly used modulations are presented in a table (they can be obtained following the same steps as for BPSK [12]).

## 4.2 Calculation of the Bit Error Probability as a function of SNIR for Binary PAM over an AWGN Channel

The following calculation follows the one in [12]. Consider a binary bipolar PAM signal, where the waveforms used to transmit information are  $f_1 = g(t)$  and  $f_2 = -g(t)$ , where  $g(t)$  is the pulse used for the transmission, with energy  $E_b = a^2 \int_0^T g^2(t) dt$  and  $g(t) \neq 0$  in the interval  $0 \leq t \leq T$ , where  $T$  is the duration of a bit. Since PAM signals are unidimensional (only the amplitude varies for different waveforms, so there is only one base function), the output of the demodulator will be a single value: the energy of the received pulse (signal plus noise)

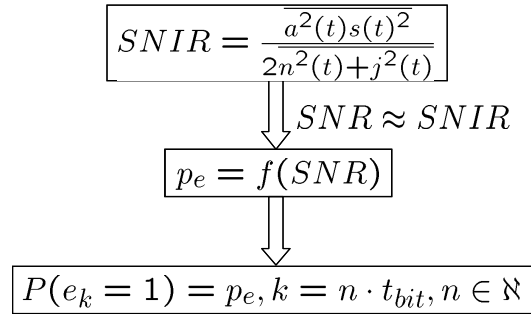


Figure 4.1: Steps for the conversion of an analog into a digital channel.

during the bit time. Notice that the binary bipolar PAM modulation under consideration here is similar to the binary PSK modulation.

Then, assuming  $f_1$  has been transmitted over an AWGN channel, the output of the demodulator is  $r = \sqrt{E_b} + n$ , where  $n$  is a Gaussian random variable with variance  $\sigma_n^2 = N_0/2$  (see Section 3.1.4 for the calculation of  $N$ ). The detector, in this case, makes a decision based on the comparison of  $r$  with the threshold 0; the probability of wrongly detecting  $f_1$  can be calculated by calculating the probability that  $r$  will have a value lower than 0 (in which case the detector would choose  $f_2$  and not  $f_1$ ).

$$\begin{aligned}
 p(r|f_1) &= \frac{1}{\sqrt{\pi N_0}} e^{-\frac{r-\sqrt{E_b}}{N_0}} \\
 P(r \leq 0|f_1) &= \int_{-\infty}^0 p(r|f_1) dr \\
 &= \frac{1}{\sqrt{2\pi}} \int_{-\infty}^0 e^{-\frac{r-\sqrt{2E_b}}{N_0}} dr \\
 &= \frac{1}{\sqrt{2\pi}} \int_{-\infty}^{-\sqrt{2E_b}/N} e^{-x^2} dx \\
 &= Q\left(\sqrt{\frac{E_b}{N}}\right),
 \end{aligned}$$

where  $Q(x) = \frac{1}{\sqrt{2\pi}} \int_x^\infty e^{-t^2/2} dt$ .

If  $f_2$  has been transmitted, the vector  $r$  would have the value  $r = -\sqrt{E_b} + n$ , and the error probability  $P(e|f_2) = P(r \geq 0|f_2)$  will have the same value as  $P(e|f_1)$ . Since  $f_1$  and  $f_2$  are equiprobable, the probability that the received waveform will produce a wrong demodulated bit is

$$\begin{aligned}
 P_e &= \frac{1}{2}P(e|f_1) + \frac{1}{2}P(e|f_2) \\
 &= Q\left(\sqrt{\frac{2E_b}{N_0}}\right).
 \end{aligned}$$

### 4.3 Calculation of the Bit Error Probability as a function of SNIR for BPSK over a Rayleigh Fading Channel

In the previous section it was assumed that the channel over which the transmission occurred was AWGN, so that the noise was modelled as a stochastic process and the signal power as a constant value. It happens often, though, that also the received signal power varies and can only be characterised as a stochastic process. To obtain the bit error probability for the communication over a channel where the received signal level is described as a random stochastic process, the probability of error over the AWGN channel has to be integrated over all the possible values of the signal, that is

$$P_{e|\text{Rayleigh}} = \int_0^\infty P_{e|\text{AWGN}}(\gamma_b) p(\gamma_b) d\gamma_b, \quad \gamma_b = E_b/N_0.$$

This is the case, for example, of a Rayleigh fading channel, described previously in Section 2.3. The energy of a pulse is in this case no longer constant, but is described by a stochastic process  $E_b = E[a_{FA}]^2 E_b|_{\text{AWGN}}$ . For a Rayleigh fading channel,  $a_{FA}$  is Rayleigh distributed, and  $a_{FA}^2$  therefore chi-square distributed, with two degrees of freedom.

$$p(\gamma_b) = \frac{1}{\bar{\gamma}_b} e^{-\gamma_b/\bar{\gamma}_b}$$
$$\bar{\gamma}_b = \frac{E_b}{N_0} E(\alpha^2)$$
$$P_{e|\text{Rayleigh}} = \frac{1}{2} \left( 1 - \sqrt{\frac{\bar{\gamma}_b}{1 + \bar{\gamma}_b}} \right)$$

The bit error probability for the communication over a Rayleigh fading channel is much higher than over an AWGN channel.

For other statistical description of the fading process, the bit error probability can be obtained by substituting the chi-square distribution by the corresponding one and integrating.

### 4.4 Results for Other Digital Modulation Schemes over an AWGN Channel

Expressions for the bit error probabilities of several binary modulations are given in Table 4.1.

Table 4.2 gives expressions for the calculation of the symbol error probabilities of multi-level modulations. Since a modulation with  $k = \log_2 M$  levels transmits  $M$  bits with a single pulse, blocks of  $M$  bits are jointly demodulated. The expressions are nevertheless in function of the energy to noise per bit relationship  $E_b$  which is calculated as  $E_b = E_S/k$ , where  $E_S$  is the energy per symbol pulse.

Modulation	Coherent Demodulation	Non-coherent Demodulation
BPSK	$Q\left(\sqrt{\frac{E_b}{N_0}}\right)$	—
DBPSK	$2Q\left(\sqrt{\frac{E_b}{N_0}}\right)$	$\frac{1}{2}e^{-E_b/N_0}$
FSK	—	$\frac{1}{2}e^{-\frac{E_b}{2N_0}}$

Table 4.1: Bit error probabilities in dependance of the per-bit energy-to-noise ratio for different binary digital modulations.

Modulation	Symbol Error Probability $P_M$	$P_b = f(P_M)$
QPSK	$2Q\left(\sqrt{\frac{2E_b}{N}}\right) \left  1 - \frac{1}{2}Q\left(\sqrt{\frac{2E_b}{N}}\right) \right $	$\frac{1}{k}P_M$
DQPSK	$\approx 4Q\left(\sqrt{\frac{E_b}{N}}\right)$	$2Q\left(0.59\frac{E_b}{N}\right)$
M-PSK	$\approx 2Q\left(\sqrt{2\log_2 M \frac{E_b}{N_0} \sin \frac{\pi}{M}}\right)$	$\approx \frac{1}{k}P_M$
M-FSK	$\sum_{n=1}^{M-1} (-1)^{n+1} \binom{M-1}{n} \frac{1}{n+1} \exp\left[-\frac{nkE_b}{(n+1)2N}\right]$	$\frac{2^{k-1}}{2^k-1}P_M$
M-PAM	$\frac{2(M-1)}{M}Q\left(\sqrt{\frac{(6\log_2 M)E_{b\,avg}}{(M^2-1)N_0}}\right) 1$	—
M-QAM	$1 - \left(1 - 2\left(1 - \frac{1}{\sqrt{m}}\right)Q\left(\sqrt{\frac{3}{M-1}\frac{E_{b\,avg}}{2N}}\right)\right)^2 2$	—

Table 4.2: Symbol error probabilities in dependance of the per-bit energy-to-noise ratio for different M-ary digital modulations.

## Chapter 5

# Conclusions

In this report analytical models were discussed, explaining the behavior of the wireless channel as it is observed in reality. The wireless channel is known for its unreliable and stochastic nature. Still, for many application scenarios it is the first choice of medium, due to the lack of alternatives.

The behavior of the wireless channel may be divided into two parts: attenuating factors and additive factors. Both contribute to the stochastic behavior of the channel. The attenuating factors, residing in the radio channel, can be analytically be decomposed into three components. One of them is deterministic and depends solely on the distance between transmitter and receiver. The other two are stochastic, but might be modeled according to their primary and secondary statistics. They depend on the propagation environment as well as on the time scale and sampling rate with which the wireless channel is observed.

The additive factors, residing in the modulation channel, may be modeled by two components, which are both stochastic. The first one, noise, is a omnipresent effect and can not be excluded from system analysis. It is not characteristic for wireless channels, but is a limiting factor in any communication system. The second source, interference, depends again on the considered scenario. Since interference is caused by devices transmitting radio frequency signals, it is important to clarify first, if these signals are transmitted within the same frequency bands or not and further how far such disturbing sources are away from the actual receiver considered. There exist multiple scenarios, where interference has no significant impact.

The analysis in this report provides a framework in order to classify different, considered transmission scenarios and determine in advance, which effects might be of interest for the specific scenario and which one not. Thus, it builds a fundamental block for simulating a certain scenario. However, turning these analytical models into running simulations requires a further step. This will be treated in a next technical report, which will use the results of this one in order to guide the reader to implementable simulation models of wireless channels.

# Bibliography

- [1] D. Apostolakis and P. Constantinou. Man made noise measurements and modelling. In *2nd International Conference on Universal Personal Communications, Personal Communications: Gateway to the 21st Century*, volume 2, pages 585–589, 1993.
- [2] K.L Blackard, T.S. Rappaport, and C. W. Bostian. Measurements and models of radio frequency impulsive noise for indoor wireless communications. *IEEE Journal on Selected Areas in Communications*, 11(7):991–1001, Sep 1993.
- [3] A. Bruce Carlson. *Communication Systems*. McGraw-Hill International Editions, 3rd edition, 1986.
- [4] J. K. Cavers. *Mobile Channel Characteristics*. Kluwer Academic Publishers, 2000.
- [5] W. C. Jakes. *Microwave Mobile Communications*, chapter 4, pages 295–298. IEEE Press, Wiley Interscience, 1994.
- [6] R. Dalke, R. Achatz, Y. Lo, P. Papazian, and G. Hufford. Measurement and analysis of man-made noise in vhf and uhf bands. In *Proceedings of Wireless Communications Conference*, pages 229–233, 1997.
- [7] M. Gudmundson. Correlation model for shadow fading in mobile radio systems. In *Electronics Letters*, volume 27, pages 2145–2146. IEEE, November 1991.
- [8] W. C. Jakes. *Microwave Mobile Communications*. IEEE Press, Wiley Interscience, 1994.
- [9] W.C.Y. Lee. *Mobile Cellular Telecommunications*. McGraw-Hill International Editions, 1995.
- [10] A. Neskovic, N. Neskovic, and G. Paunovic. Modern approaches in modeling of mobile radio systems propagation environment. *IEEE Communications Surveys and Tutorials*, Third Quarter 2000.
- [11] Y. Oda, R. Tsuchihashi, K. Tsunekawa, and M. Hata. Measured path loss and multipath propagation characteristics in uhf and microwave frequency bands for urban mobile communications. In IEEE, editor, *Proceedings of the 53rd IEEE Vehicular Technology Conference — VTC 2001*, volume 1, pages 337–341, 2001.
- [12] J. G. Proakis. *Digital Communications*. McGraw-Hill International, 4 edition, 2001.

- [13] Theodore S. Rappaport. *Wireless Communications*. Prentice Hall, 1999.
- [14] S. Y. Seidel and T. S. Rappaport. 900 mhz path loss measurements and prediction techniques for in-building communication system design. In *Proceedings of the 41st IEEE Vehicular Technology Conference*, pages 613–618, 1991.
- [15] S. Y. Seidel, T. S. Rappaport, and R. Singh. Path loss and multipath delay statistics in four european cities for 900 mhz cellular and microcellular communications. In *Electronics Letters*, volume 26, pages 1713–1715. IEEE, Sep 1990.
- [16] G.L. Siqueira, G.L. Ramos, and R.D. Vieira. Propagation measurements of a 3.5 ghz signal: Path-loss and variability studies. In *Proceedings of the SBMO/IEEE MTT-S International Microwave and Optoelectronics Conference — IMOC 2001*, pages 209–212, 2001.
- [17] R. Steele. *Mobile Radio Communications*. Pentech Press, 1992.
- [18] R. Steele and L. Hanzo, editors. *Mobile Radio Communications*. J. Wiley & Sons Ltd, 2000.
- [19] S. C. Yang. *CDMA RF System Engineering*. Mobile Communications Series. Artech House Publishers, 1998. page 19.
- [20] J. Zander and S.-L. Kim. *Radio Resource Managements for Wireless Networks*. Mobile Communications Series. Artech House Publishers, 2001. page 330.
- [21] X. Zhao, J. Kivinen, P. Vainikainen, and K. Skog. Propagation characteristics for wide-band outdoor mobile communications at 5.3 ghz. *IEEE Journal on Selected Areas in Communications*, 20(3):507–514, Apr 2002.